

**Analysis of NOAA aircraft data for plume studies in Northeast Texas
during TexAQS 2000**

Final report for
East Texas Council of Governments
3800 Stone Road
Kilgore, TX 75662

under Subcontract to
ENVIRON International Corporation
101 Rowland Way, Suite 220
Novato, CA 94945

William G Vizueté
University of Texas – Austin
J.J. Pickle Research Campus
Center for Energy Resources
10100 Burnett Rd. bldg 133
Austin, TX 78758
vizueté@che.utexas.edu
October 7, 2002

ACKNOWLEDGEMENTS

David Allen - University of Texas-Austin

Paul Guthrie - ENVIRON International Corporation

Donna Sueper - National Oceanic and Atmospheric Administration (NOAA)

Greg Yarwood - ENVIRON International Corporation

TABLE OF CONTENTS

INTRODUCTION	2
DATA SOURCES	2
PLUME CONCENTRATIONS	3
SUMMARY	38

INTRODUCTION

During the summer of 2000 as part of the Texas Air Quality study (TexAQS 2000), several instrumented aircraft made measurements throughout eastern Texas. Missions flown by these aircraft were operated by the National Oceanic and Atmospheric Administration (NOAA) and the National Center for Atmospheric Research (NCAR). The data that was collected by these aircraft will be used in this study to investigate ozone productivities of point sources in northeast Texas. For this analysis data that was specifically collected by the Lockheed Electra aircraft will be used. In particular, the September 3, 2000 data when the aircraft flew transects of power plants in the rural areas north of the Houston urban core. The data from this flight will be studied to calculate the ozone productivities observed in these plumes. These observed ozone productivities can be compared to ozone model results under similar meteorological conditions. The following tables give details about the aircraft and the instrumentation that was used to collect this data set:

DATA SOURCES

Aircraft: Lockheed Electra

Operated: NCAR Research Aircraft Facility / NOAA Aeronomy Laboratory

Aircraft Specifications:

Endurance: 6 hrs
Ceiling: 7.6 km
Payload: >2700 kg
Research Speed: 100-150 m/s

Aircraft Instrument Package

Parameter	Time Resolution	Method	Det. Limit
Ozone (O ₃)	10 s	UV Absorption	1 ppb
Fast O ₃ (FO ₃)	1 s	NO/O ₃ Chemiluminescence	0.2 ppb
Fast CO (FCO)	1 s	VUV Resonance Fluorescence	1 ppb
Carbon Dioxide (CO ₂)	< 1 s	NDIR	0.2 ppm
Sulfur Dioxide (SO ₂)	2 s	UV Pulsed Fluorescence	1 ppb
Nitric Oxide (NO)	1 s	NO/O ₃ Chemiluminescence	30 ppt
Nitrogen Dioxide (NO ₂)	3 s	Photolysis, NO/O ₃ Chem.	100 ppt
Total Nitrogen Oxides (NO _y)	1 s	Au Converter, NO/O ₃ Chem.	50 ppt

PAN	1 s / every 6 min	Dir. Injection, GC/ECD	< 5 ppt
PPN	1 s / every 6 min	Dir. Injection, GC/ECD	< 5 ppt
MPAN	1 s /every 6 min	Dir. Injection, GC/ECD	< 5 ppt
Nitric Acid (HNO ₃)	1 s	C I Mass Spectrometry	10 ppt
NH ₃	5 s	C I Mass Spectrometry	50 ppt
In-situ VOCs	1 min./every 15 min	Cryo Collection, GC/FID	< 10 ppt
Canister VOCs	< 1 min.	Canister Sampling, GC/MS	< 10 ppt
CH ₂ O		Liquid Chromatography	
Peroxides (incl. H ₂ O ₂)	1 min	Dual Enzymatic / Fluorimeter	30 ppt
Aerosol size distribution	1 s	NMASS	5 - 90 nm
Aerosol size distribution	1 s	ERAST	70 - 1000 nm
Total Radiation	1 s	Eppley Pyranometers - Zenith & Nadir	0.28 - 2.8 μ
UV Radiation	~10 s	Spectral Radiometer - Zenith & Nadir	295 - 480 nm
Visible Radiation		Visible Absorption Spectrometer	420 - 700 nm
Water Vapor (H ₂ O)	1 s	Lyman Alpha Absorption	
Air Temperature	1 s	Platinum Thermistor	
Dewpoint/Frostpoint	< 3 s	Chilled Mirror	
Wind Speed	1 s	Derived from INE	
Wind Direction	1 s	Derived from INE	
Altitude	1 s	Barometric	
Position	1 s	GPS, INE	
Air Speed	1 s	Barometric	
Biometer		3-wavelength IR Absorption	
Atmospheric Reflectivity		C & X Band Radars	

PLUME CONCENTRATIONS

The Electra aircraft flew transects of power plant plumes found in the rural areas north of Houston on September 3, 2000. On this day the Electra aircraft took off late in the afternoon for a plume and isoprene chemistry flight across east Texas. The aircraft followed a north to south track beginning just north (upwind) of the Monticello power

plant and proceeding with parallel transects across and south (downwind) of the Martin Lake power plant. The flight path on this day is illustrated in figure 1.

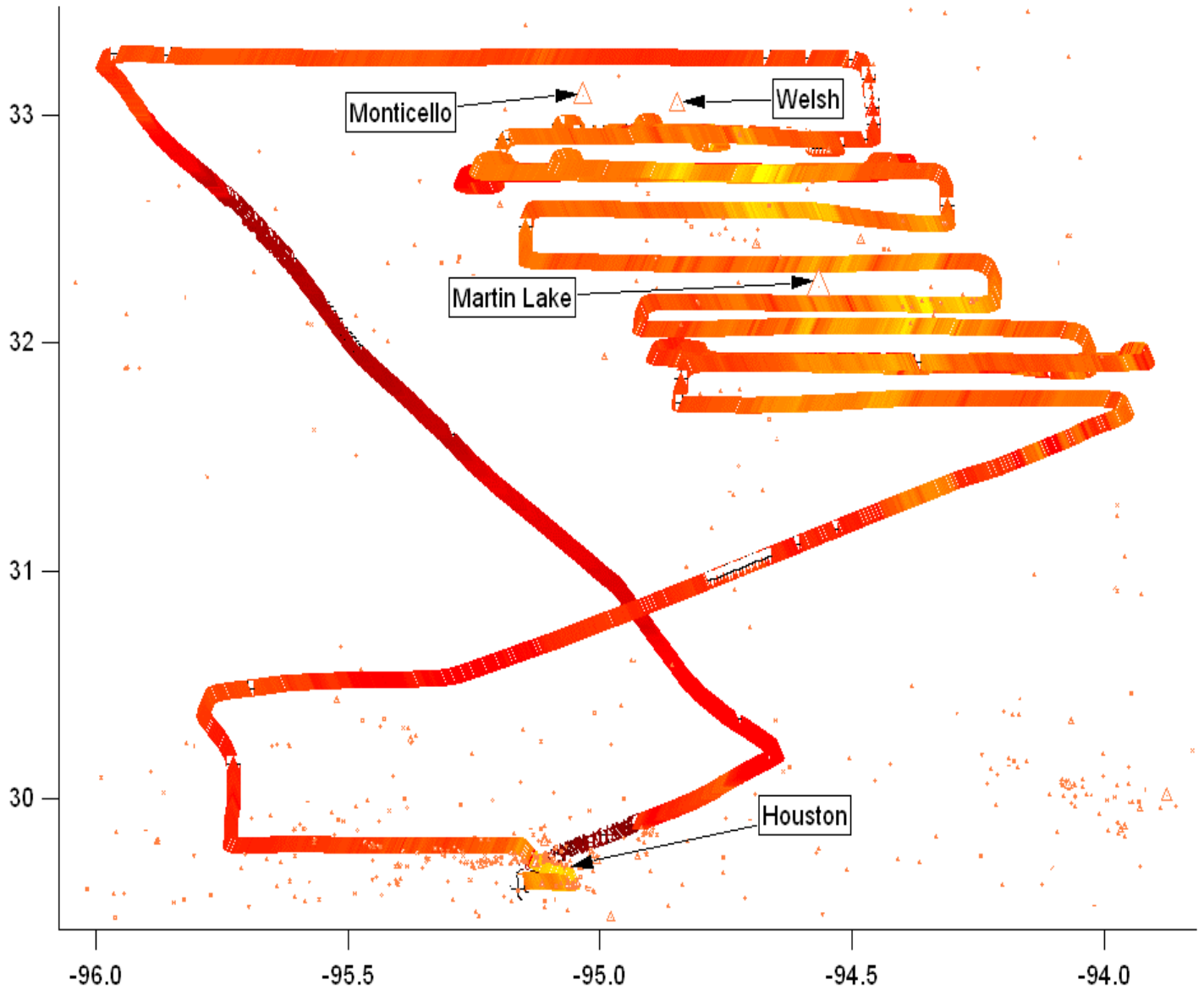


Figure 1. Flight path of Electra aircraft on September 3, 2000. The aircraft initially flew east from Houston and returns flying east into Houston.

All aircraft data was accessed via an ftp site maintained by NOAA. The site address is <ftp.al.noaa.gov>. All available aircraft data at the ftp site are in an Igor *.bwav format. Therefore, analysis of the data required the use of the Igor Pro software version 4.0.5.1 by Wavemetrics www.wavemetrics.com. The following figures show the 1-second NOy,

SO₂ and ozone concentration data that was collected from the aircraft during its flight on September 3rd.

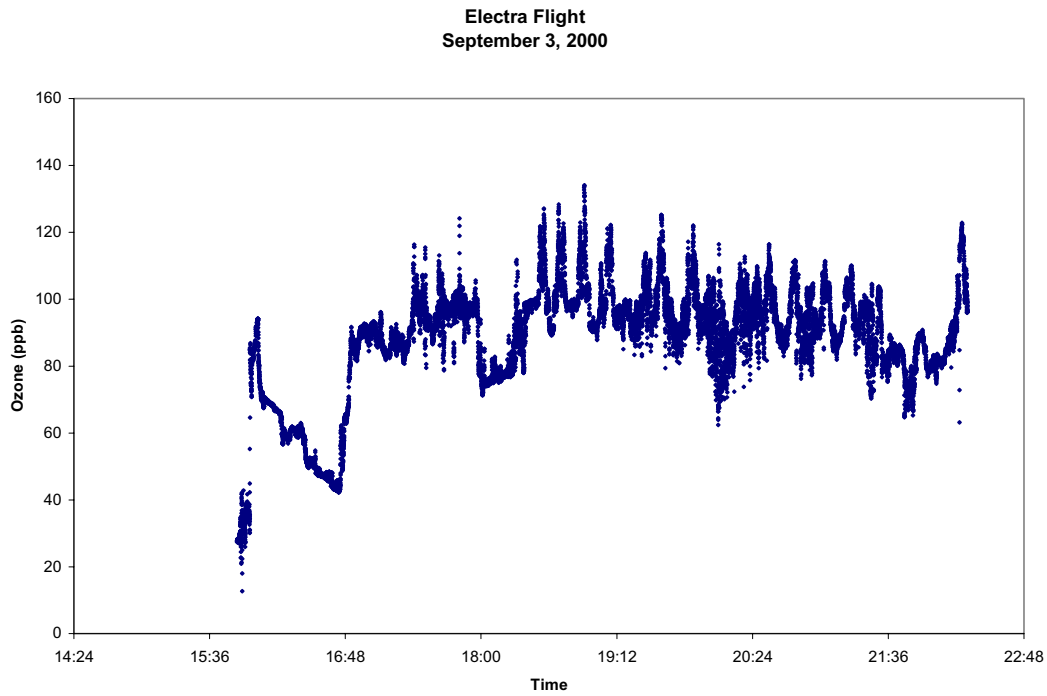


Figure 2. Ozone concentrations (one second data) for September 3, 2000 Electra flight.

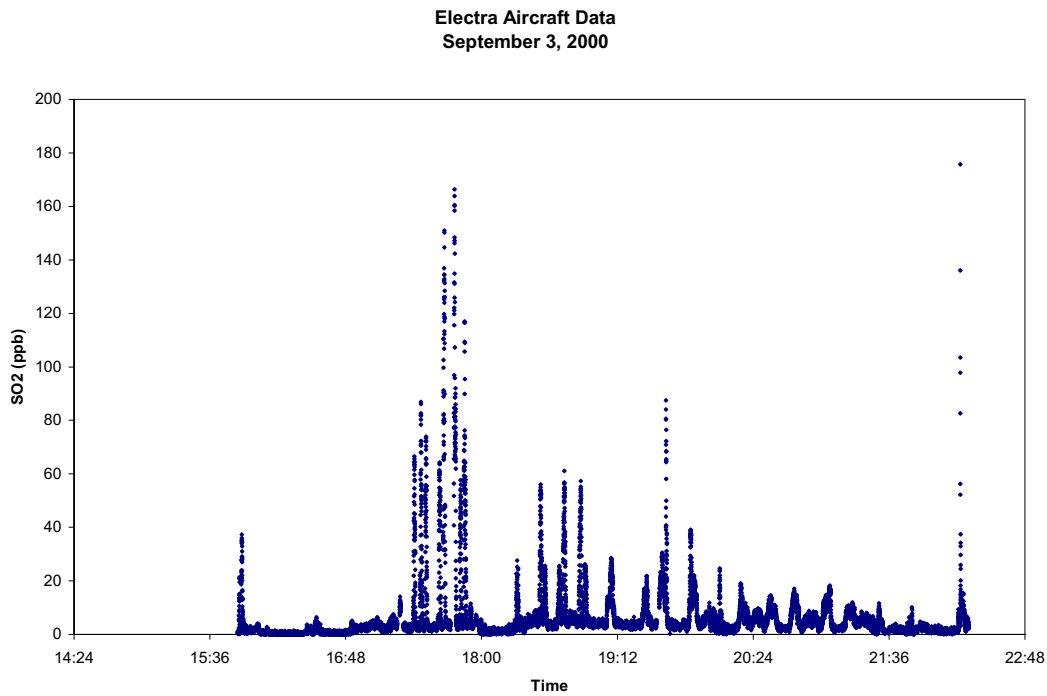


Figure 3. SO₂ concentrations (one second data) for September 3, 2000 Electra flight.

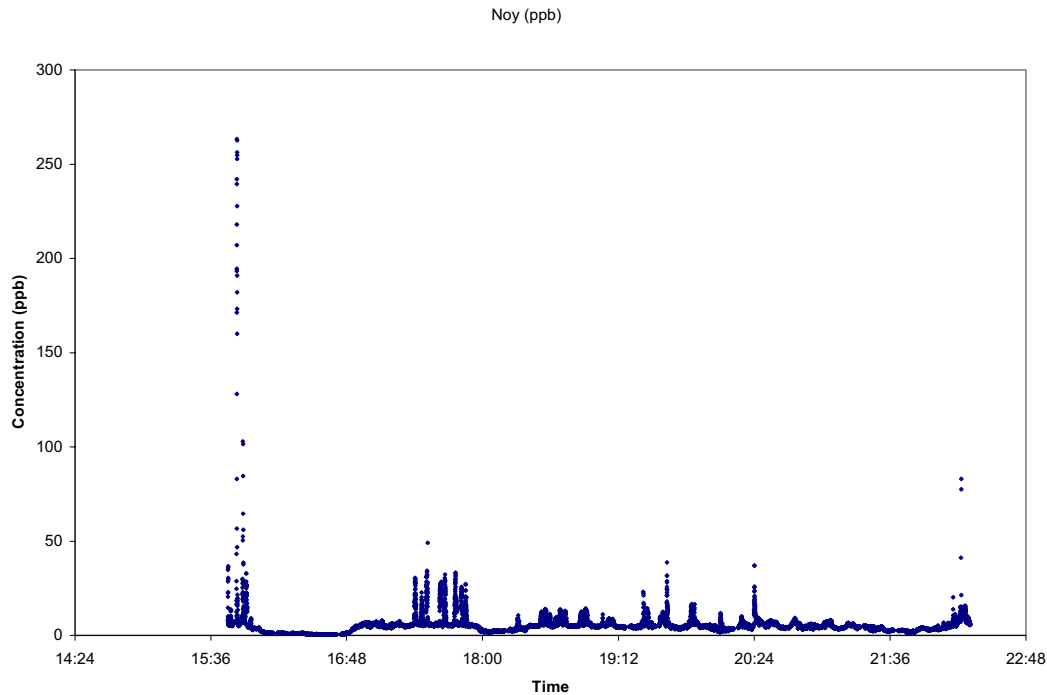


Figure 4. NO_y concentrations (one second data) for September 3, 2000 Electra flight.

While the aircraft was in transit from Houston the altitude of the aircraft was approximately 3.5 km. This high altitude accounts for the low ozone values obtained by the aircraft's instruments around 16:48.

The time series and aircraft location data was used to identify peak SO₂ concentrations. Peaks were chosen if they occurred downwind of large NO_x point sources such as the Monticello, Welsh, or Martin lake power plants. A total of 18 peak SO₂ episodes were chosen. These maxima, the flight path, and NO_x point sources are shown in figure 5. In the figure the color scale represents ozone concentration along the flight path. The thickness of the line indicates the magnitude of the SO₂ concentration. The circles locate NO_x point sources whose magnitude is indicated by the diameter of the circle.

The following table gives the altitude of the aircraft during each peak episode as well as the wind speed and direction.

Peak	NACA Pressure Altitude (m)	Wind Speed (m/s)	Wind Direction
1	647 - 660	0.8 - 5.8	282 - 359 (W - N)
2	597 - 636	0.5 - 5.2	282 - 358 (W - N)
3	638 - 653	2.0 - 6.0	300 - 6 (NW - N)
4	641 - 684	0.6 - 5.2	300 - 14 (NW - N)
5	638 - 656	1.5 - 5.7	290 - 13 (NW - NE)
6	639 - 674	2.8 - 7.1	307 - 360 (NW - N)
7	606 - 677	1.6 - 5.2	295 - 33 (NW - NE)
8	647 - 677	0.2 - 6.3	299 - 14 (NW - N)
9	816 - 845	2.1 - 7.8	292 - 3 (NW - N)
10	483 - 524	1.8 - 6.9	285 - 25 (NW - NE)
11	302 - 331	1.0 - 6.9	278 - 8 (W - N)
12	657 - 680	3.2 - 7.7	322 - 13 (NW - N)
13	301 - 321	3.0 - 9.7	299 - 30 (NW - NE)
14	653 - 689	1.8 - 6.7	289 - 4 (NW - N)
15	651 - 684	1.8 - 6.2	291 - 15 (NW - N)
16	649 - 680	4.2 - 9.1	299 - 15 (NW - N)
17	652 - 684	4.0 - 8.5	315 - 20 (NW - NE)
18	654 - 710	1.7 - 10.2	310 - 45 (NW - NE)

Background ozone, SO₂, and NO_y concentrations from the transit upwind of Monticello ranged from 83.5 – 96.1 ppb, 0.7 – 5.5 ppb, and 3.9 – 7.8 ppb respectively.

The aircraft data was also compared to ozone concentrations collected at three monitoring stations located near the aircraft’s flight path. The following lists information about each monitoring station including the observed hourly averaged ozone concentrations. All data was taken from the Texas Commission on Environmental Quality (www.tceq.state.tx.us).

Monitor: Longview (C19/C127)

Latitude: 32° 22' 57" North (+32.382500°)

Longitude: 94° 42' 45" West (-94.712500°)

Monitor Data

Time Ozone (ppb)

21:00 35

22:00 34

From airplane

Time Ozone (ppb)

21:30 82

Monitor: Longview Big Woods (C605)

Latitude: 32° 37' 04" North (+32.617778°)

Longitude: 94° 46' 44" West (-94.778889°)

Monitor Data

Time	Ozone (ppb)
------	-------------

18:00	74
-------	----

19:00	54
-------	----

20:00	42
-------	----

From airplane

Time	Ozone (ppb)
------	-------------

19:01	91
-------	----

Monitor: Cypress River Airport (C50)

Latitude: 32° 44' 34" North (+32.742778°)

Longitude: 94° 18' 12" West (-94.303333°)

Monitor Data

Time	Ozone (ppb)
------	-------------

17:00	88
-------	----

18:00	68
-------	----

19:00	47
-------	----

From airplane

Time	Ozone (ppb)
------	-------------

18:40	98.51
-------	-------

18:55	108.52
-------	--------

Figures 6 through 23 show the ozone, NO_y, and SO₂ concentrations for each of the 18 peaks. Figures 24 through 40 show scatter plots of ozone and SO₂ versus NO_y concentrations for each of the 18 peaks.

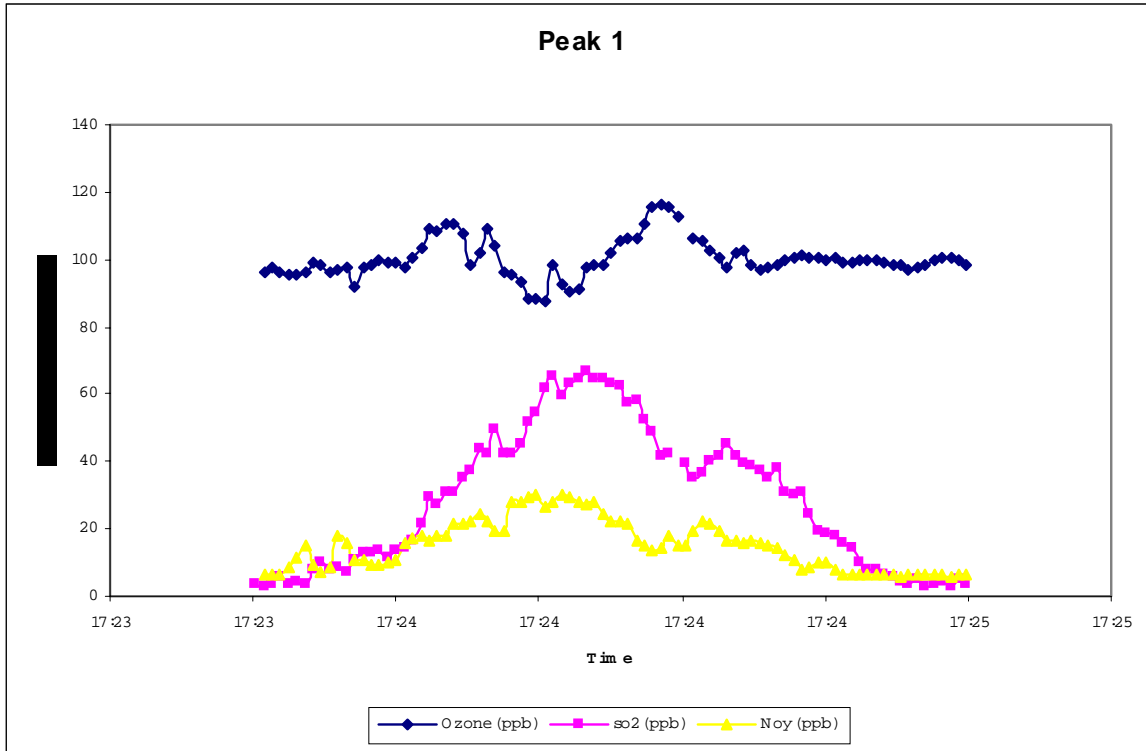


Figure 6. Ozone, NO_y, and SO₂ concentrations surrounding SO₂ peak one.

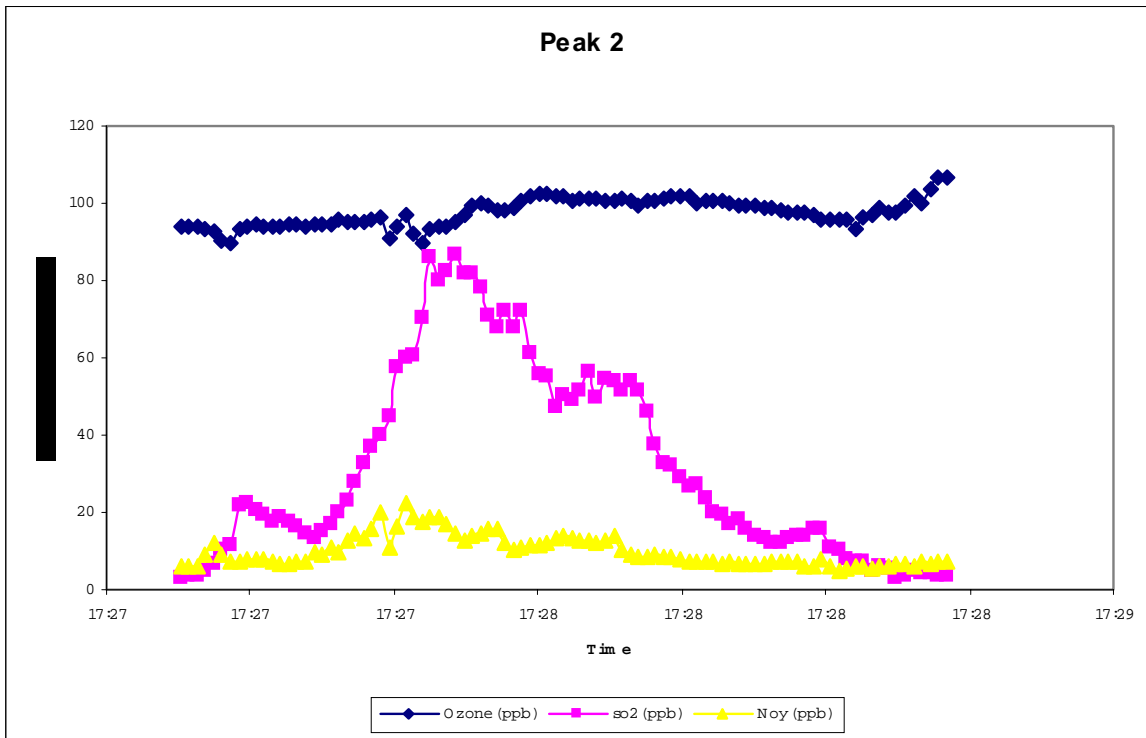


Figure 7. Ozone, NO_y, and SO₂ concentrations surrounding SO₂ peak two.

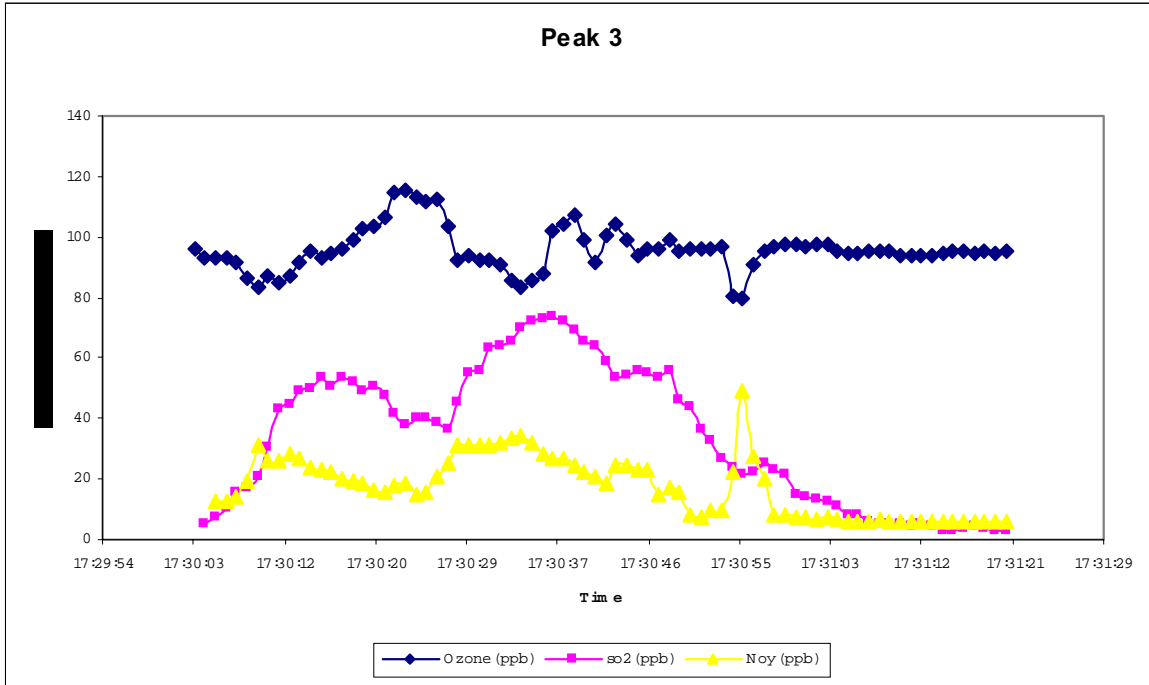


Figure 8. Ozone, NO_y, and SO₂ concentrations surrounding SO₂ peak three.

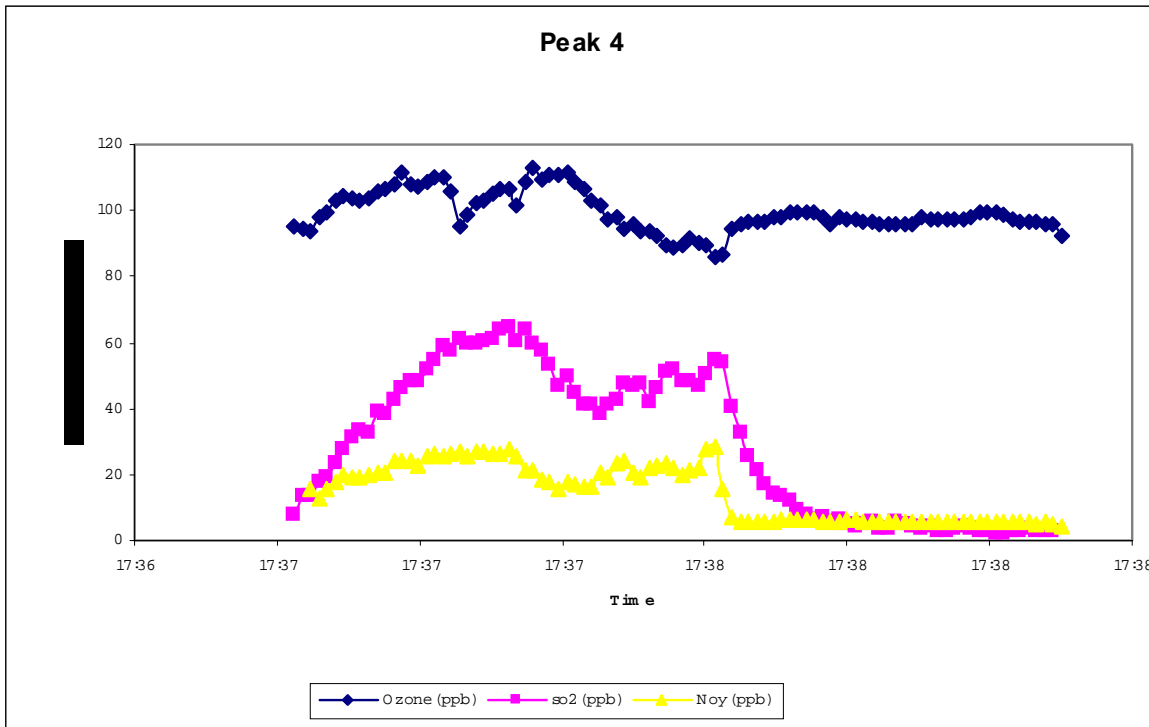


Figure 9. Ozone, NO_y, and SO₂ concentrations surrounding SO₂ peak four.

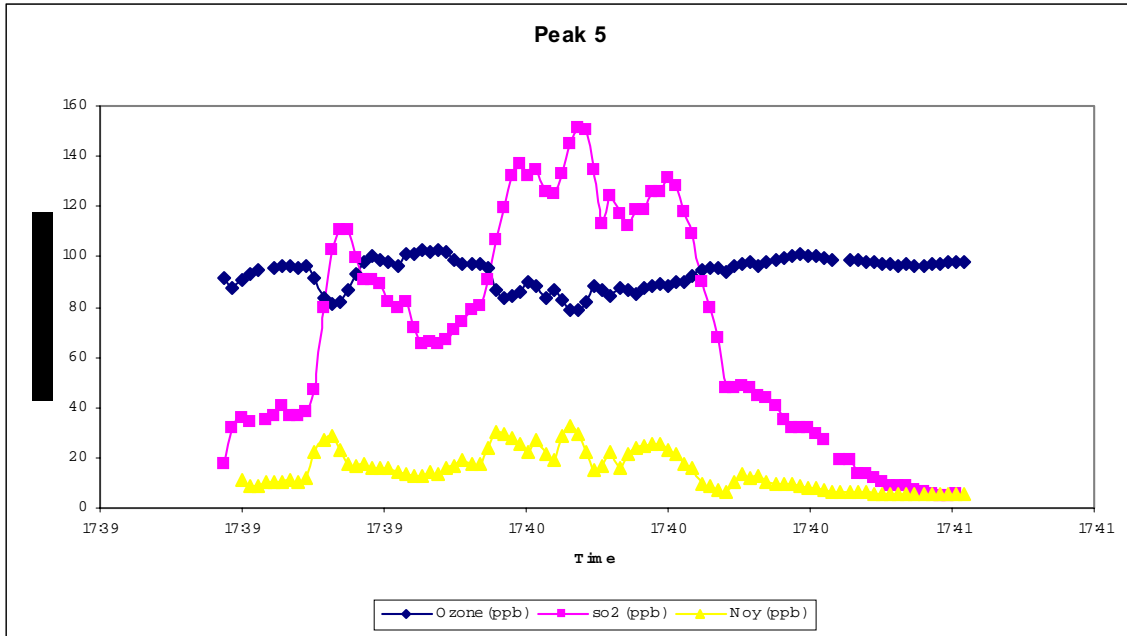


Figure 10. Ozone, NO_y, and SO₂ concentrations surrounding SO₂ peak five.

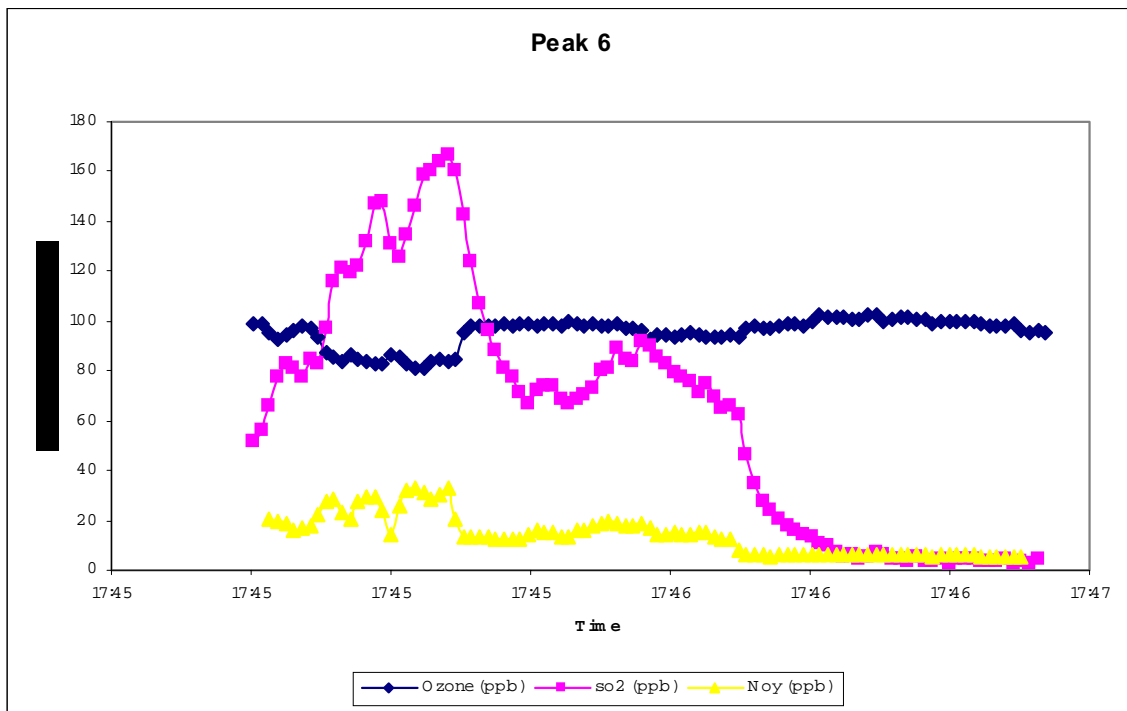


Figure 11. Ozone, NO_y, and SO₂ concentrations surrounding SO₂ peak six.

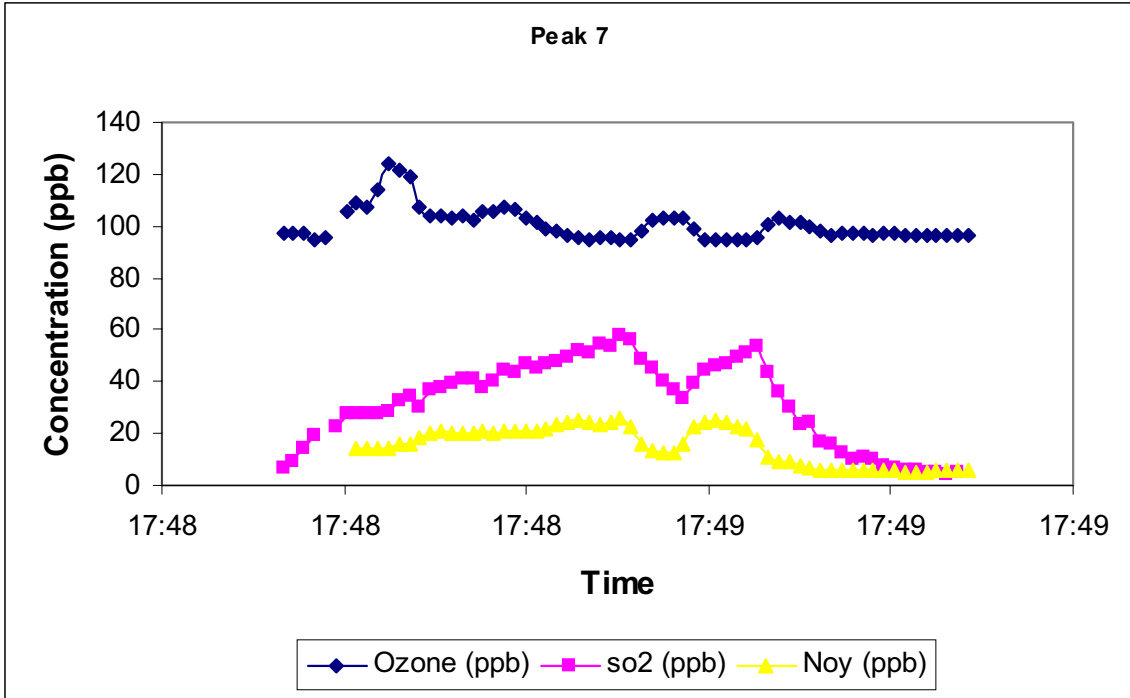


Figure 12. Ozone, NO_y, and SO₂ concentrations surrounding SO₂ peak seven.

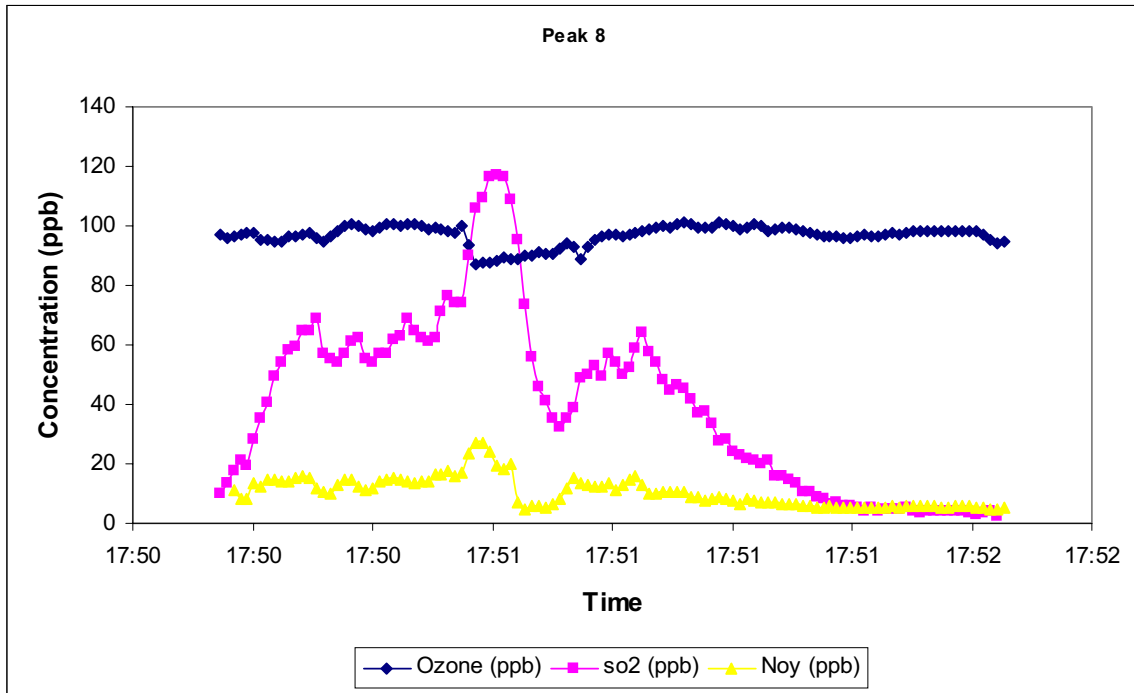


Figure 13. Ozone, NO_y, and SO₂ concentrations surrounding SO₂ peak eight.

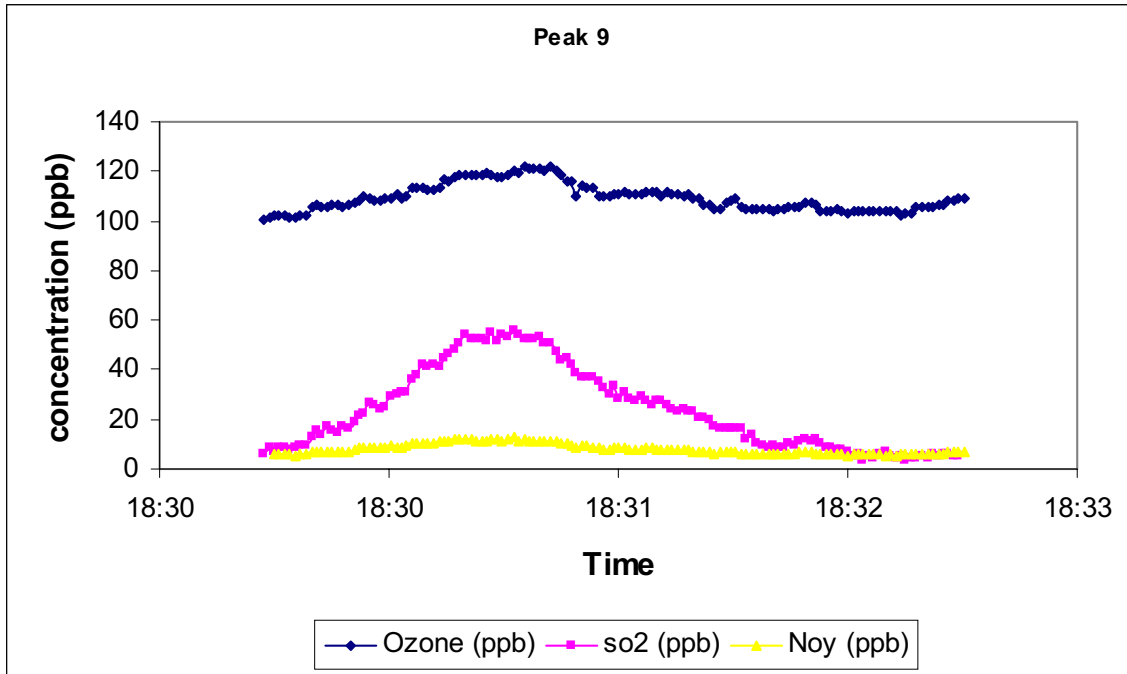


Figure 14. Ozone, NO_y, and SO₂ concentrations surrounding SO₂ peak nine.

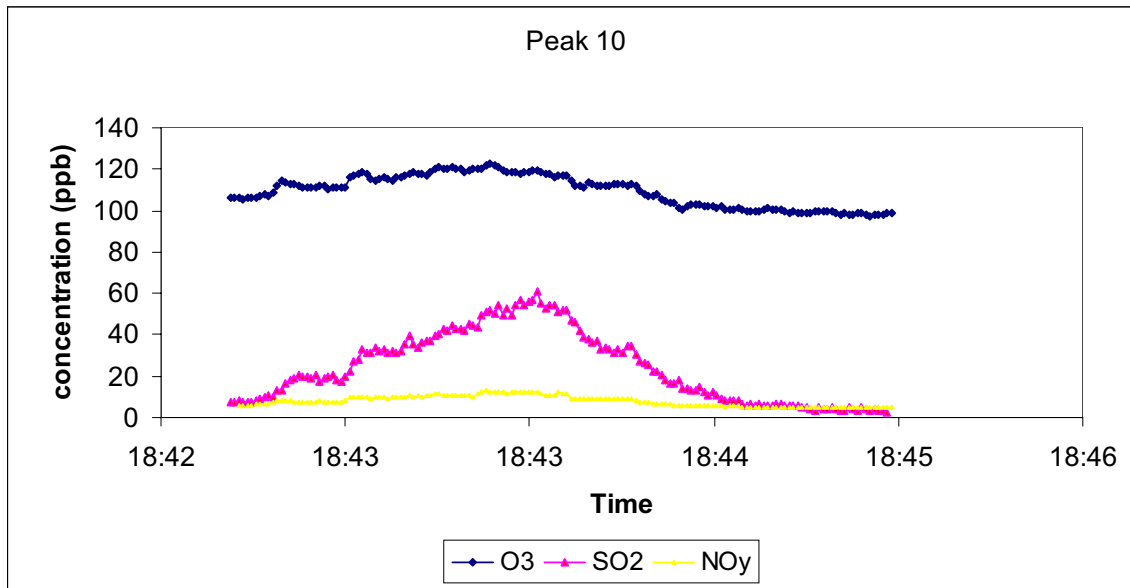


Figure 15. Ozone, NO_y, and SO₂ concentrations surrounding SO₂ peak 10.

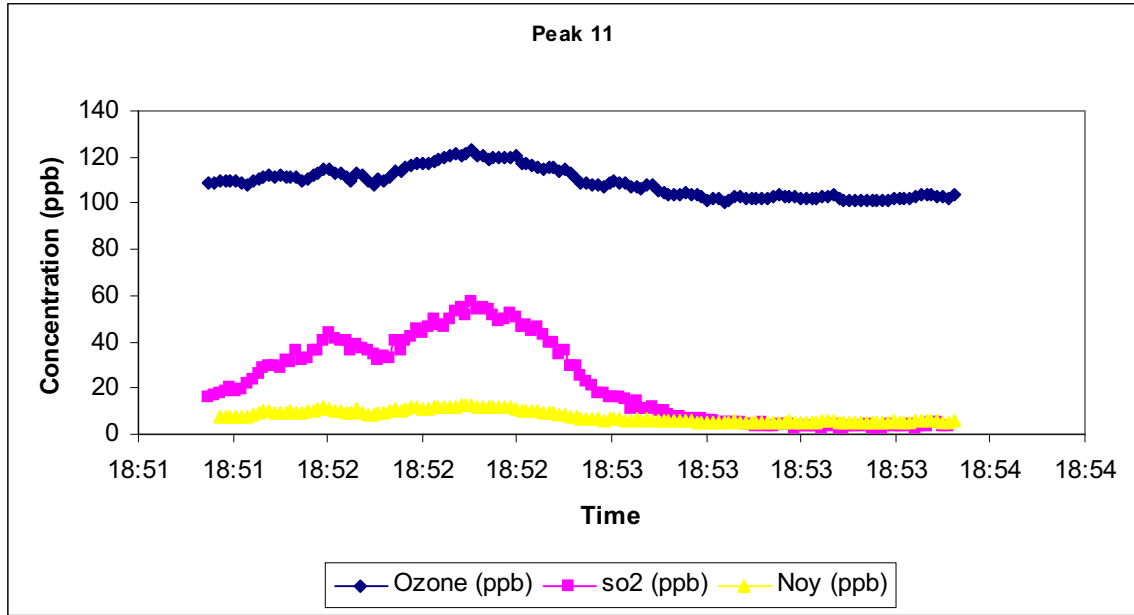


Figure 16. Ozone, NOy, and SO₂ concentrations surrounding SO₂ peak 11.

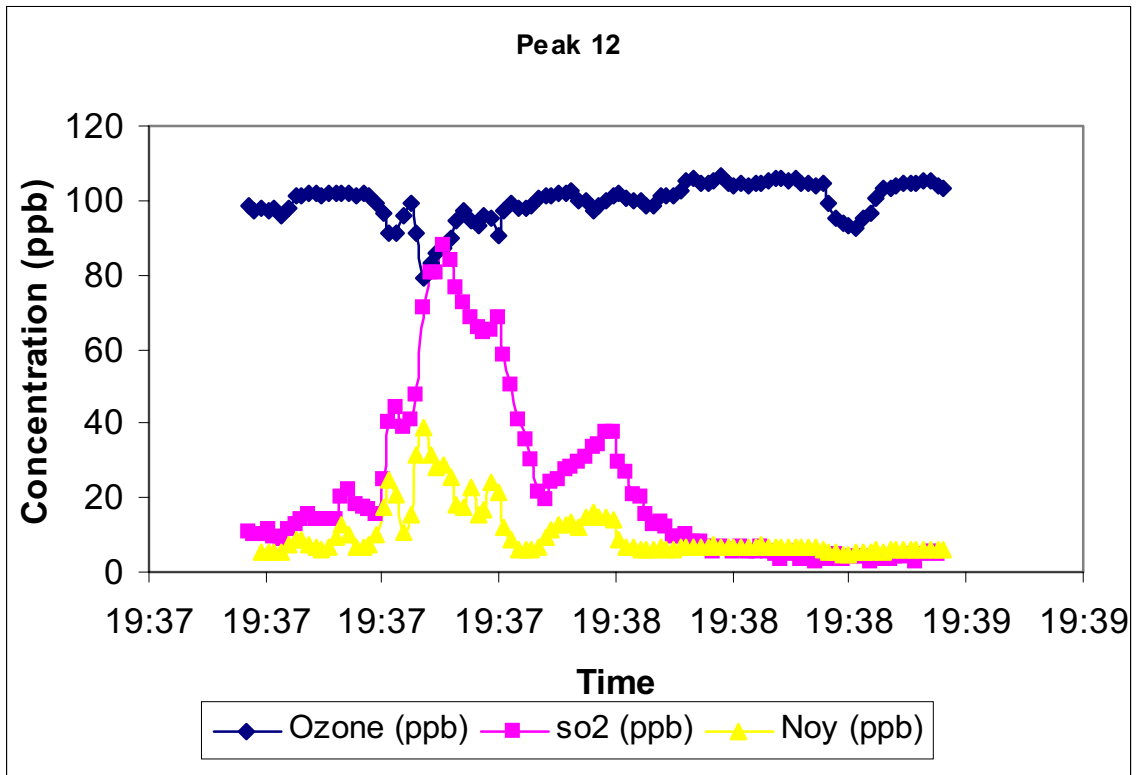


Figure 17. Ozone, NOy, and SO₂ concentrations surrounding SO₂ peak 12.

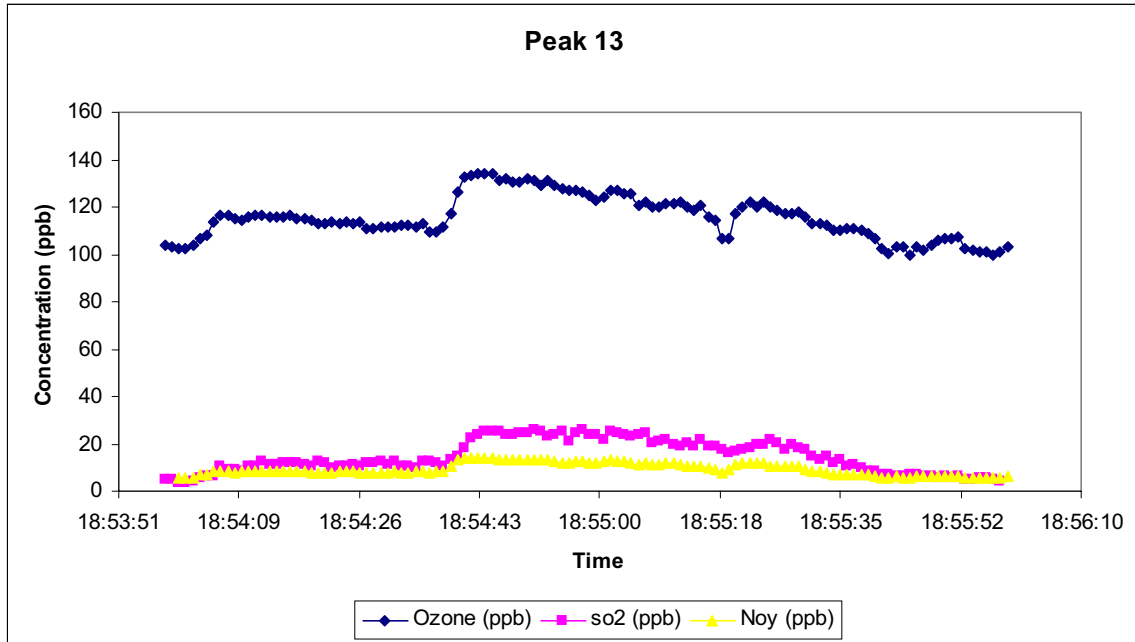


Figure 18. Ozone, NO_y, and SO₂ concentrations surrounding SO₂ peak 13.

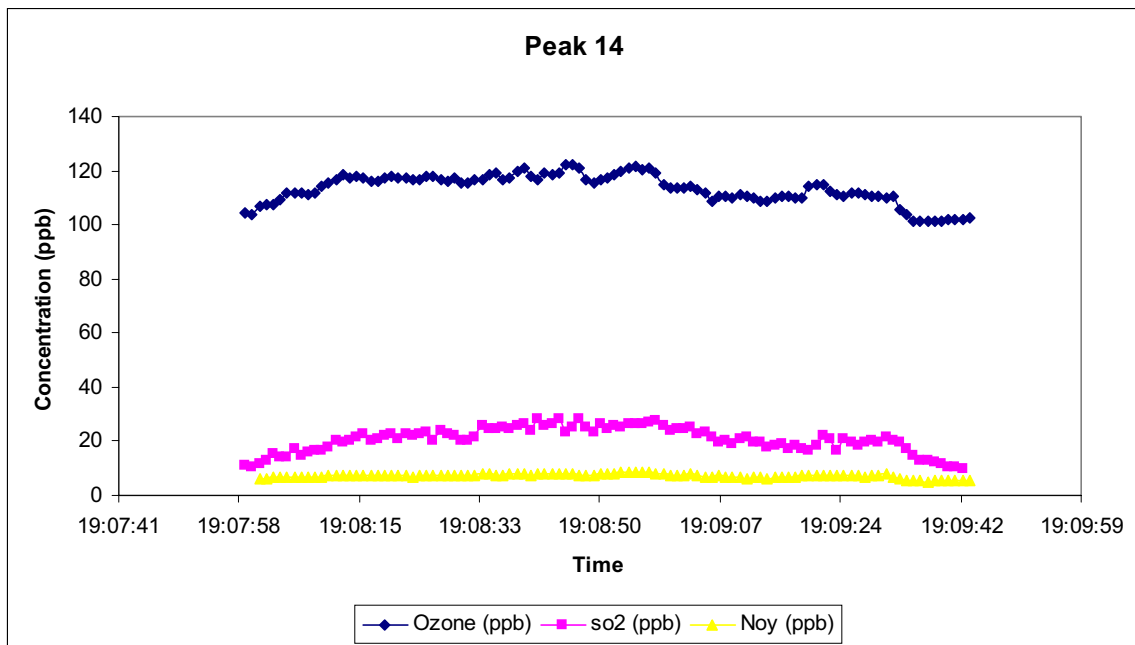


Figure 19. Ozone, NO_y, and SO₂ concentrations surrounding SO₂ peak 14.

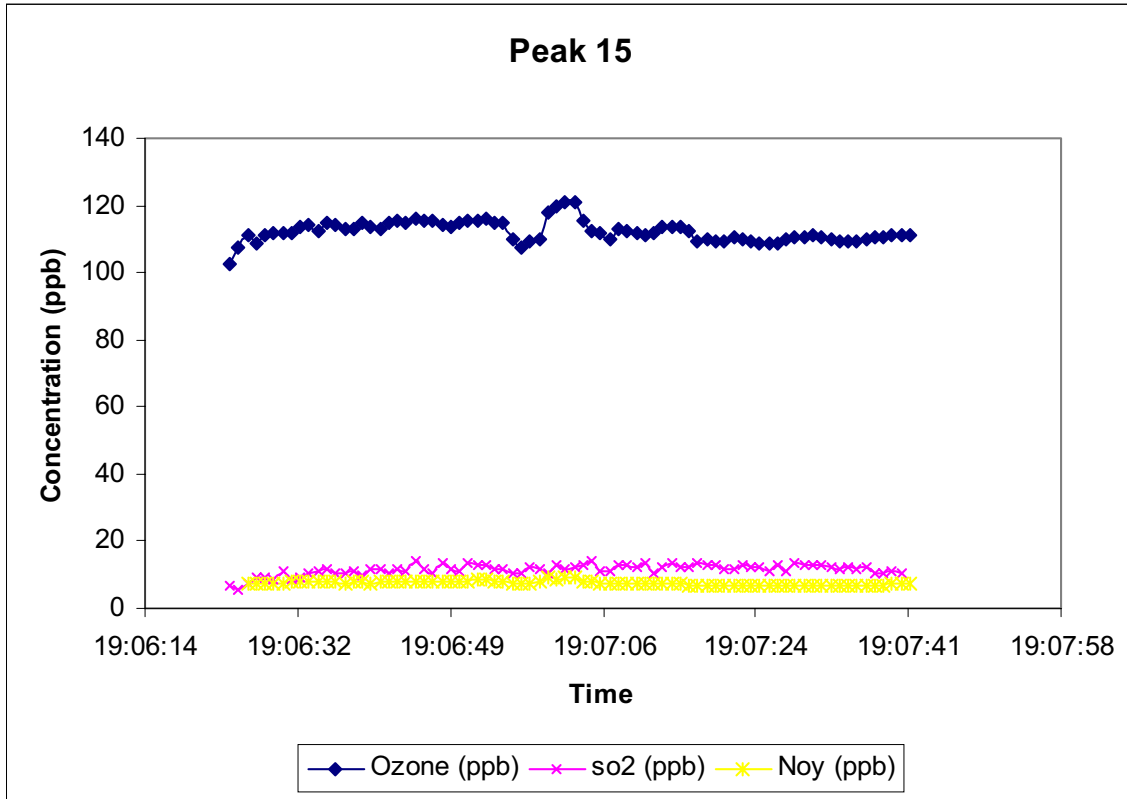


Figure 20. Ozone, NO_y, and SO₂ concentrations surrounding SO₂ peak 15.

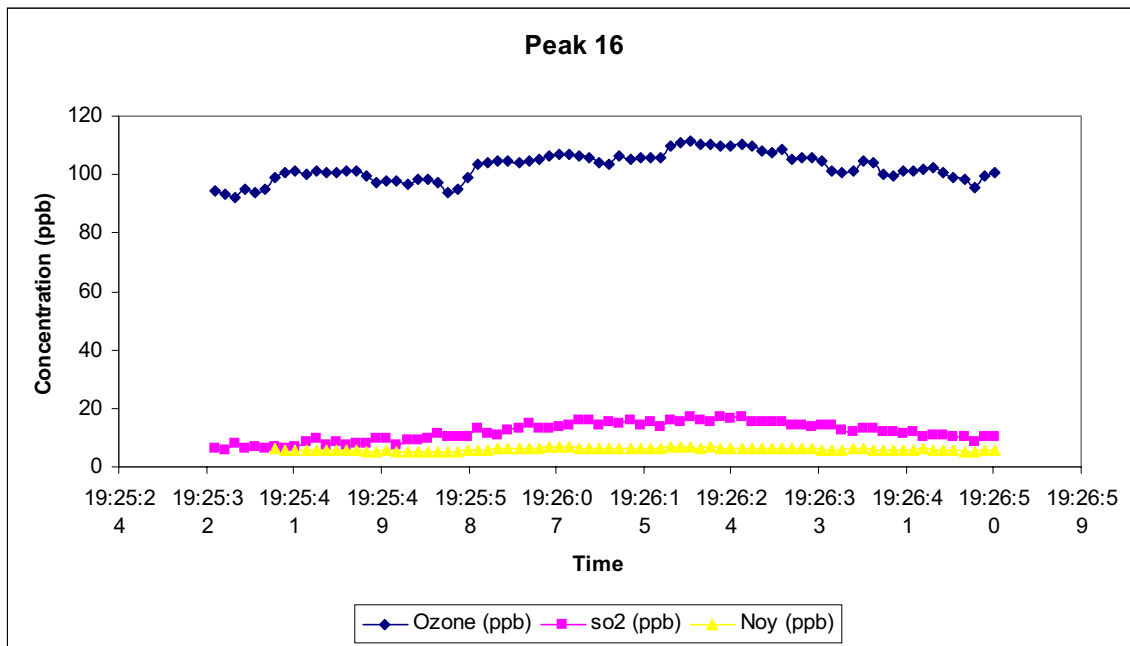


Figure 21. Ozone, NO_y, and SO₂ concentrations surrounding SO₂ peak 16

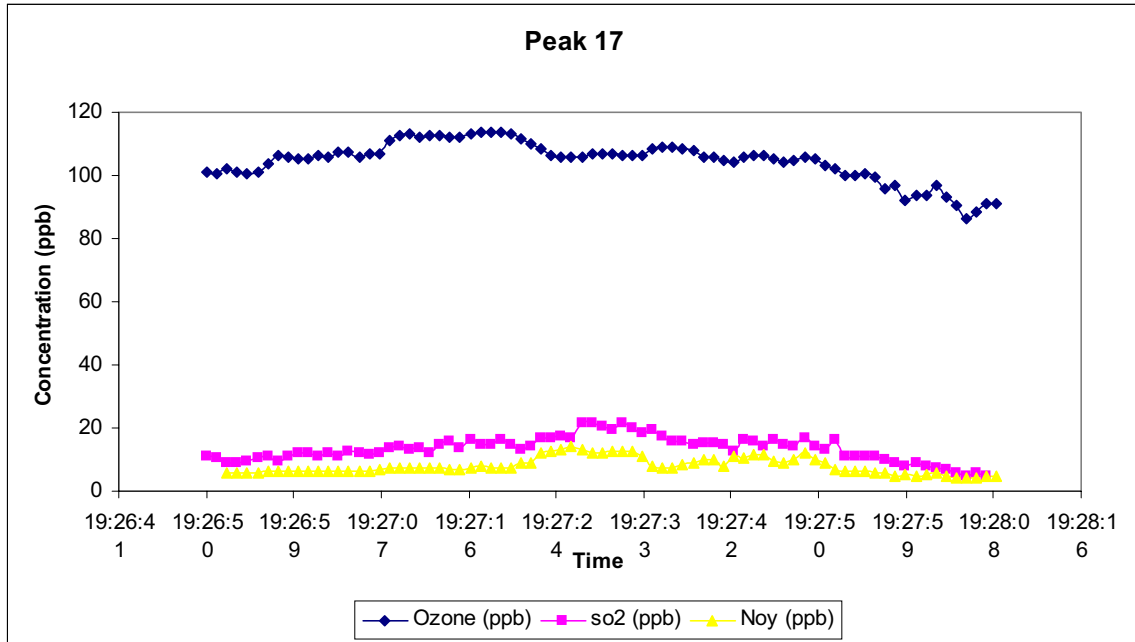


Figure 22. Ozone, NOy, and SO₂ concentrations surrounding SO₂ peak 17

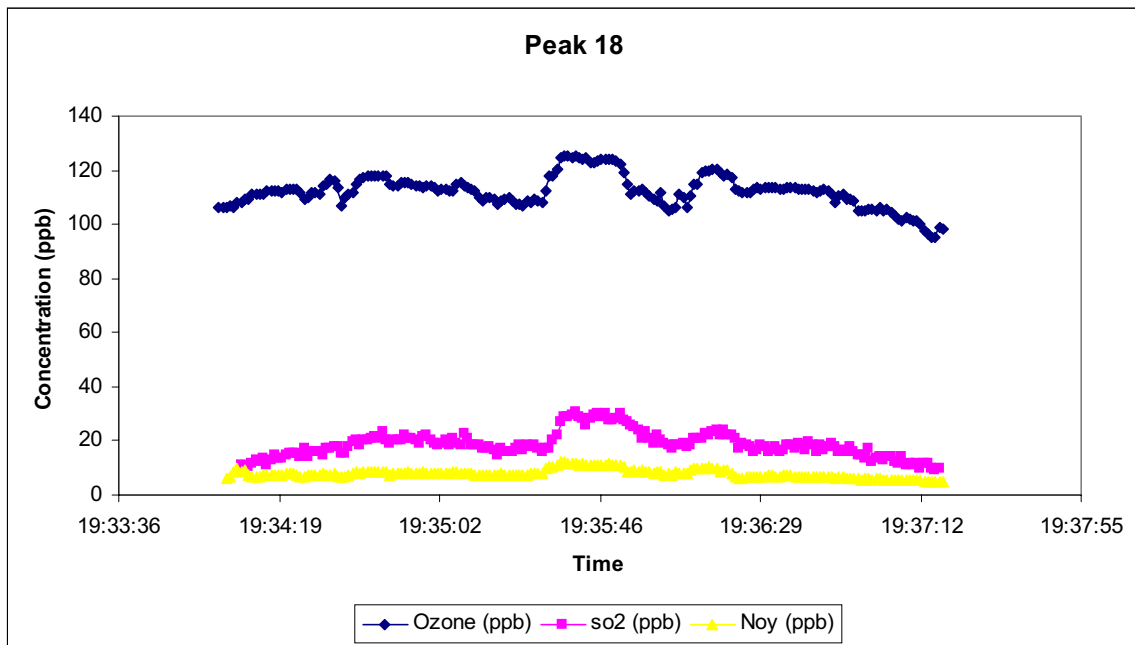


Figure 23. Ozone, NOy, and SO₂ concentrations surrounding SO₂ peak 18

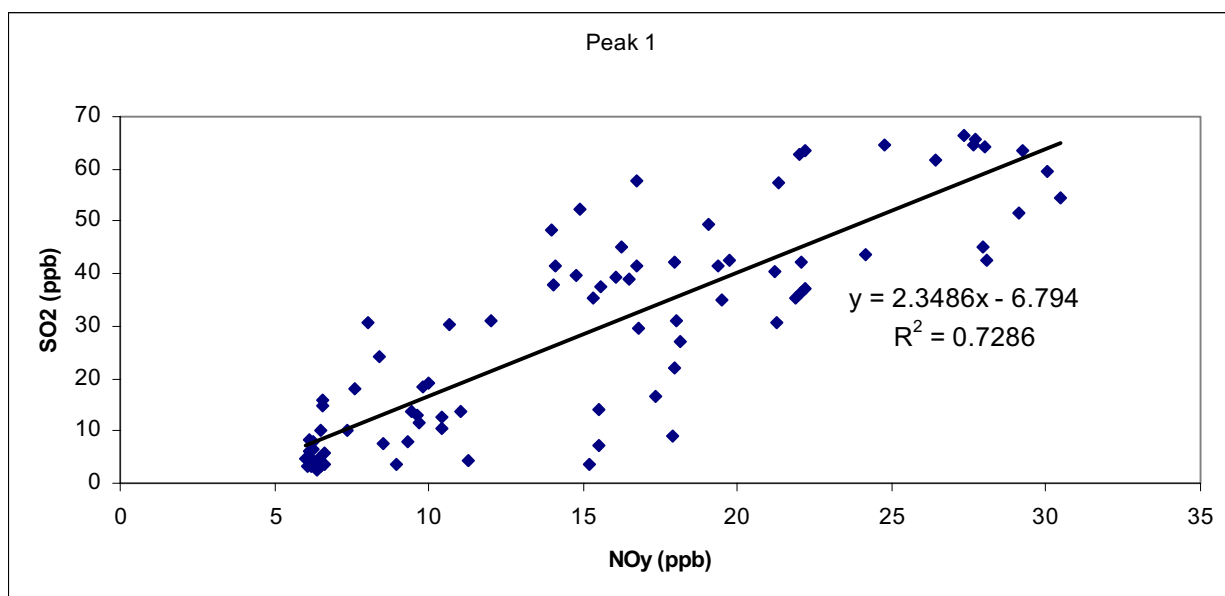
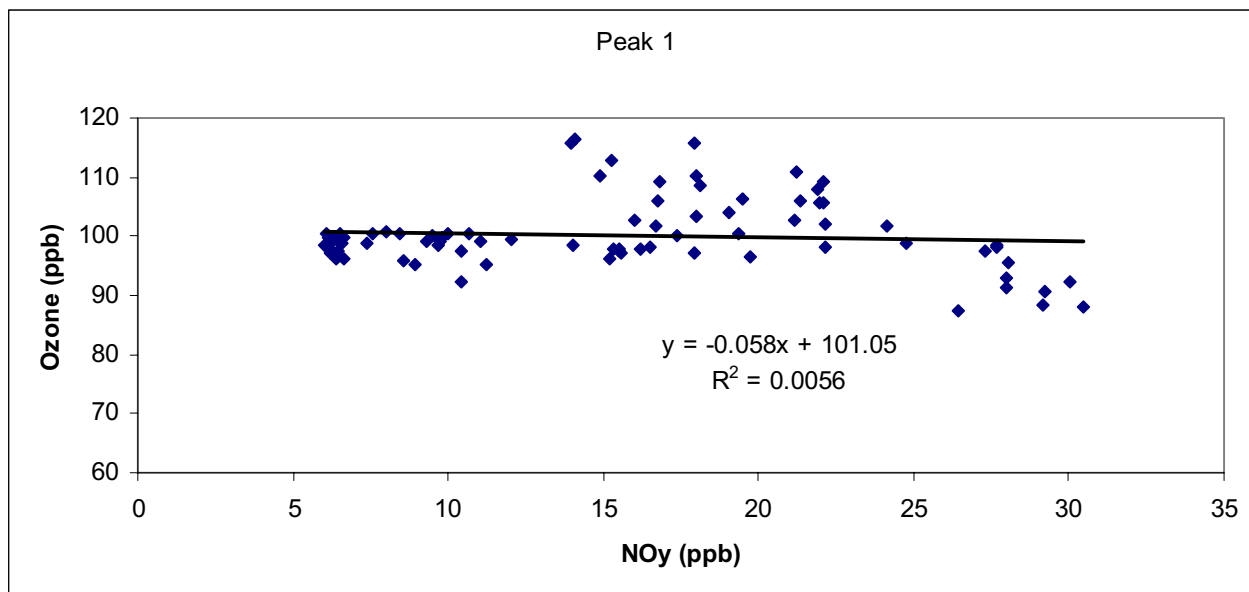


Figure 24. Scatter plots of ozone and SO₂ versus NO_y concentrations for peak 1.

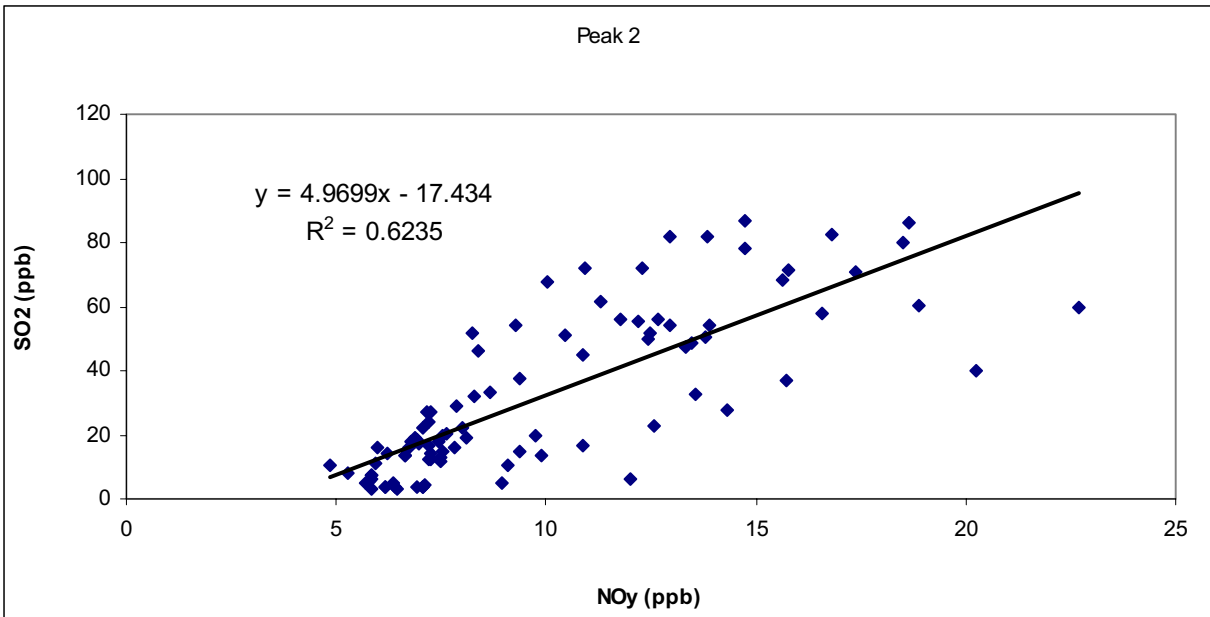
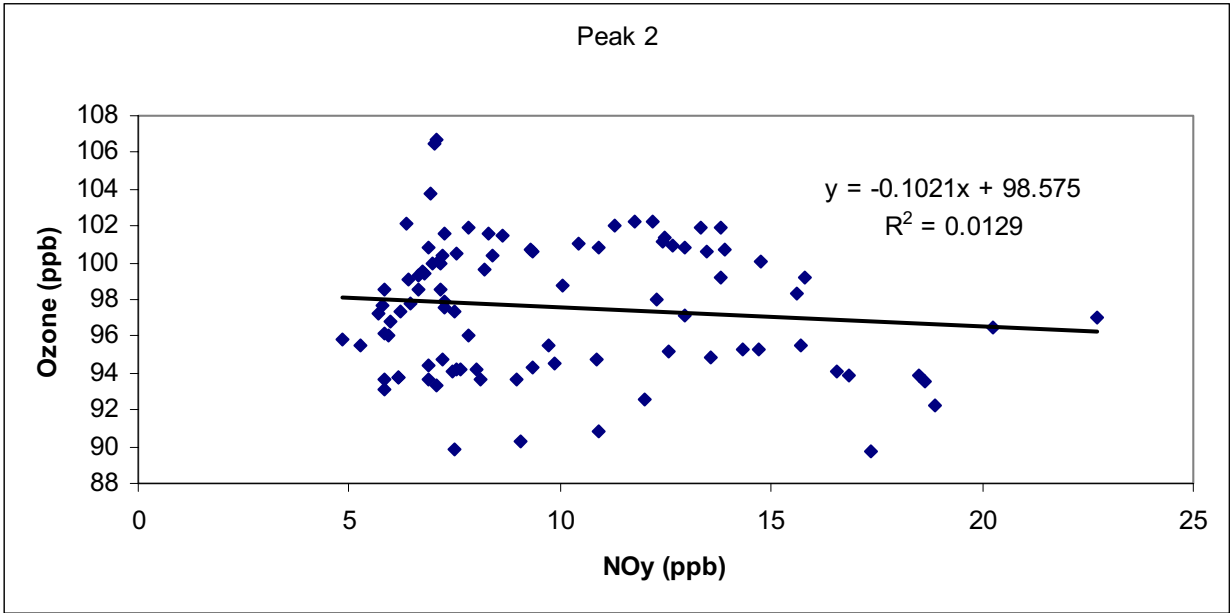


Figure 25. Scatter plots of ozone and SO₂ versus NO_y concentrations for peak 2.

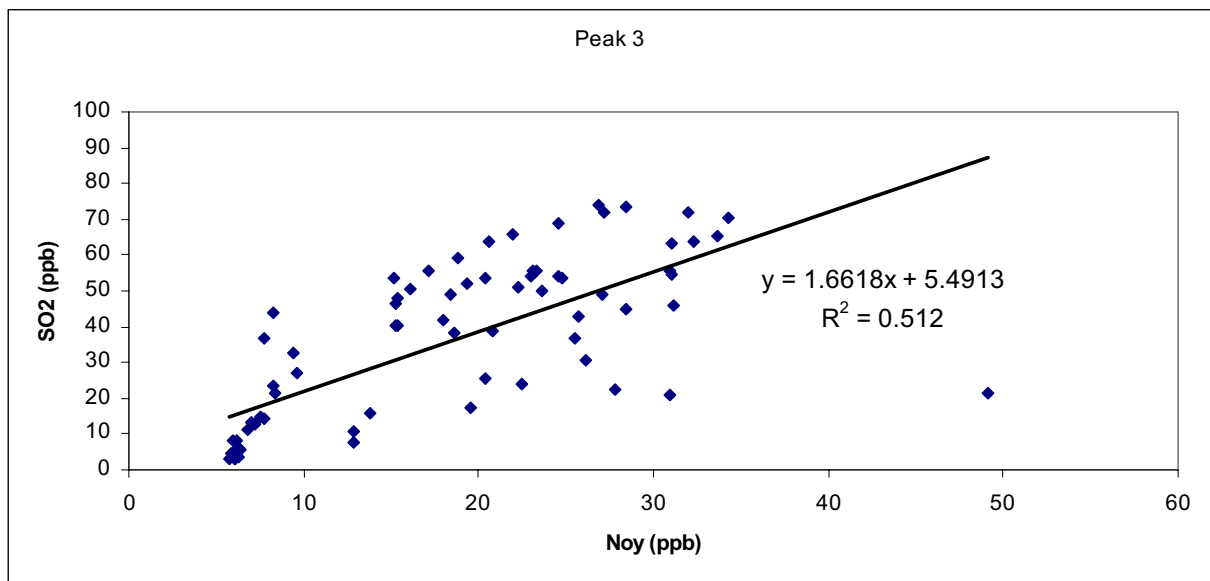
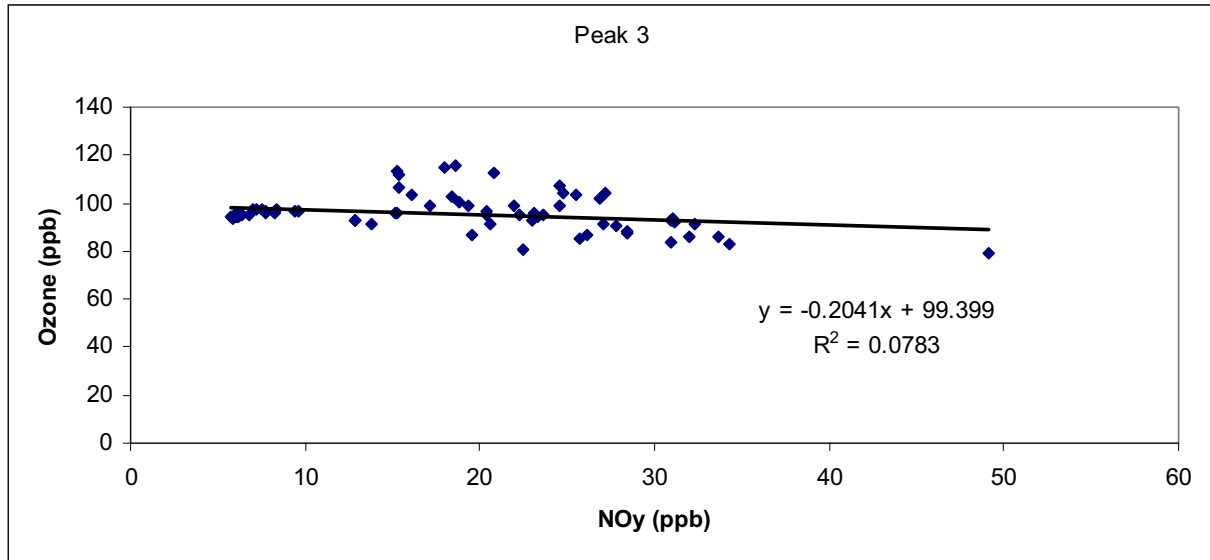


Figure 26. Scatter plots of ozone and SO₂ versus NO_y concentrations for peak 3.

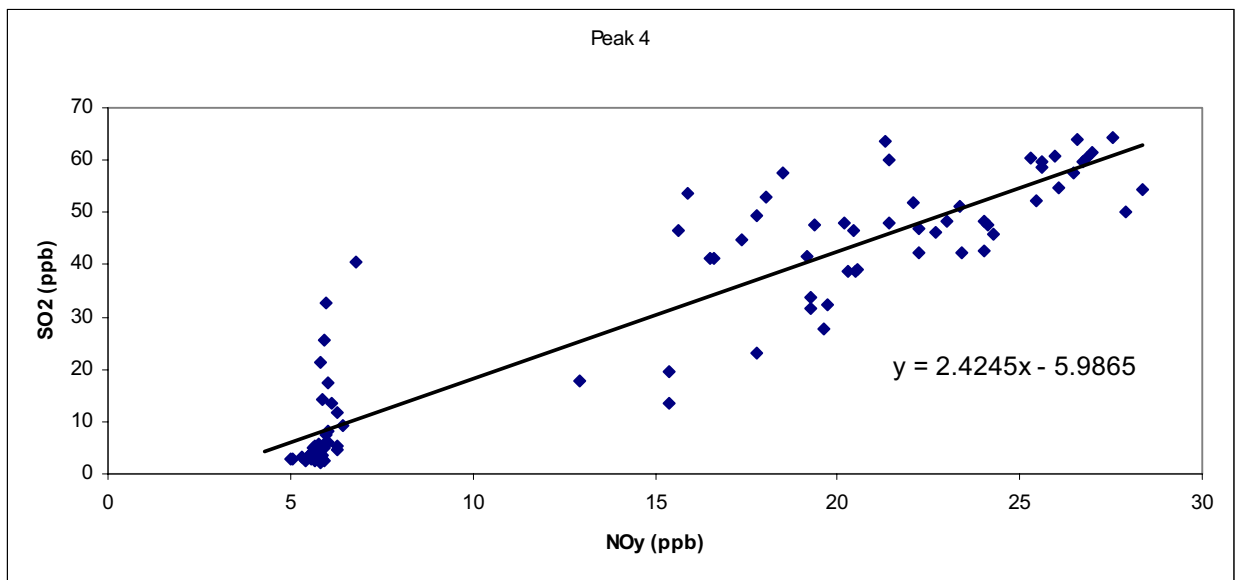
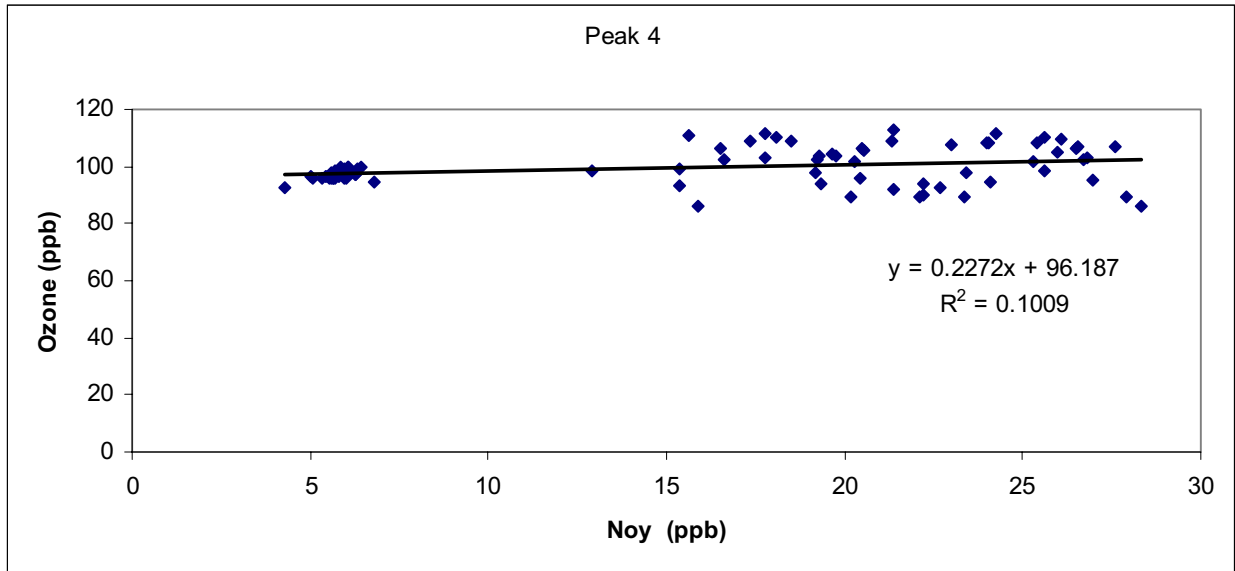


Figure 27. Scatter plots of ozone and SO₂ versus NO_y concentrations for peak 4.

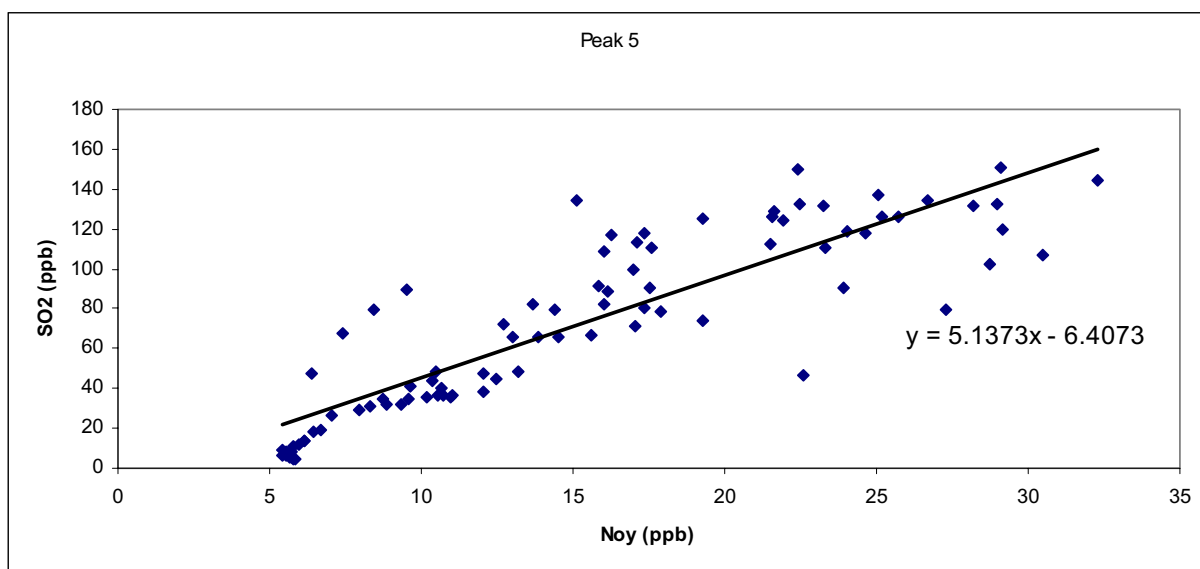
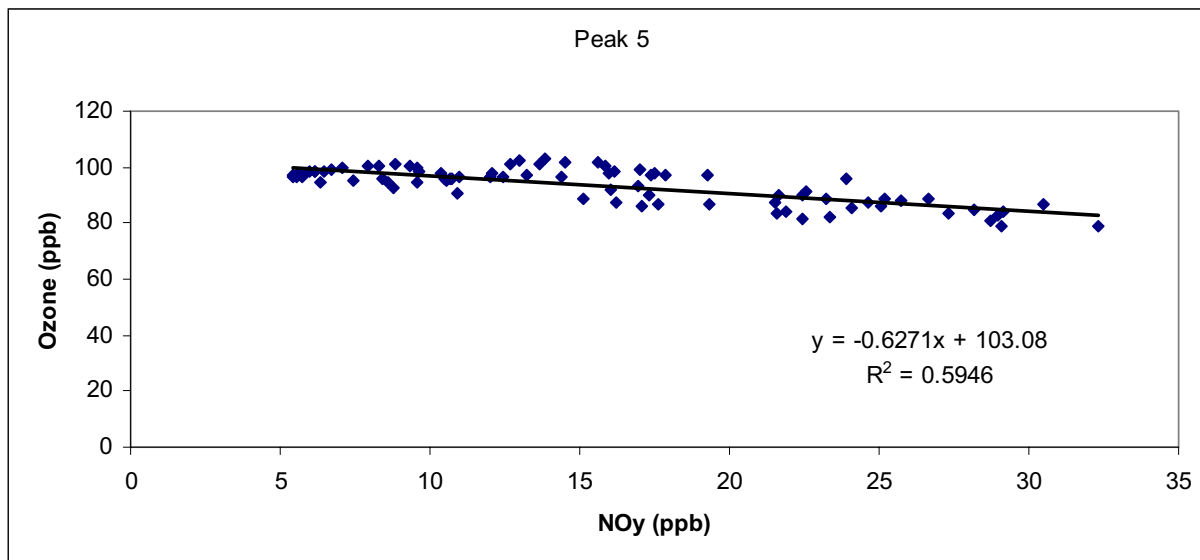


Figure 28. Scatter plots of ozone and SO₂ versus NO_y concentrations for peak 5.

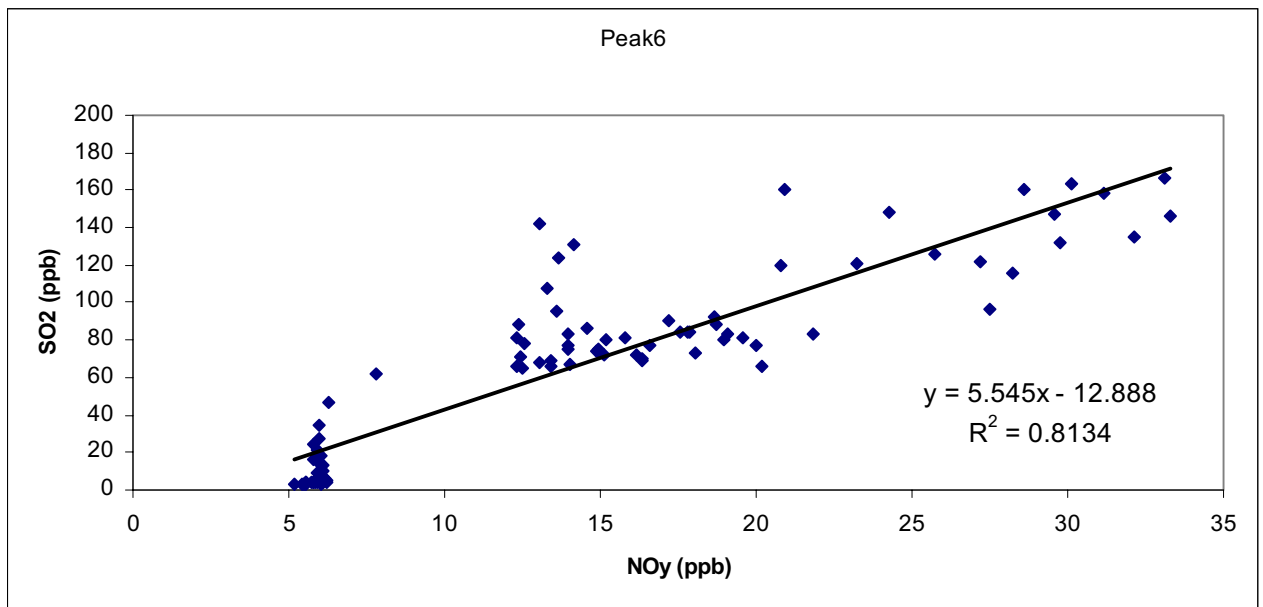
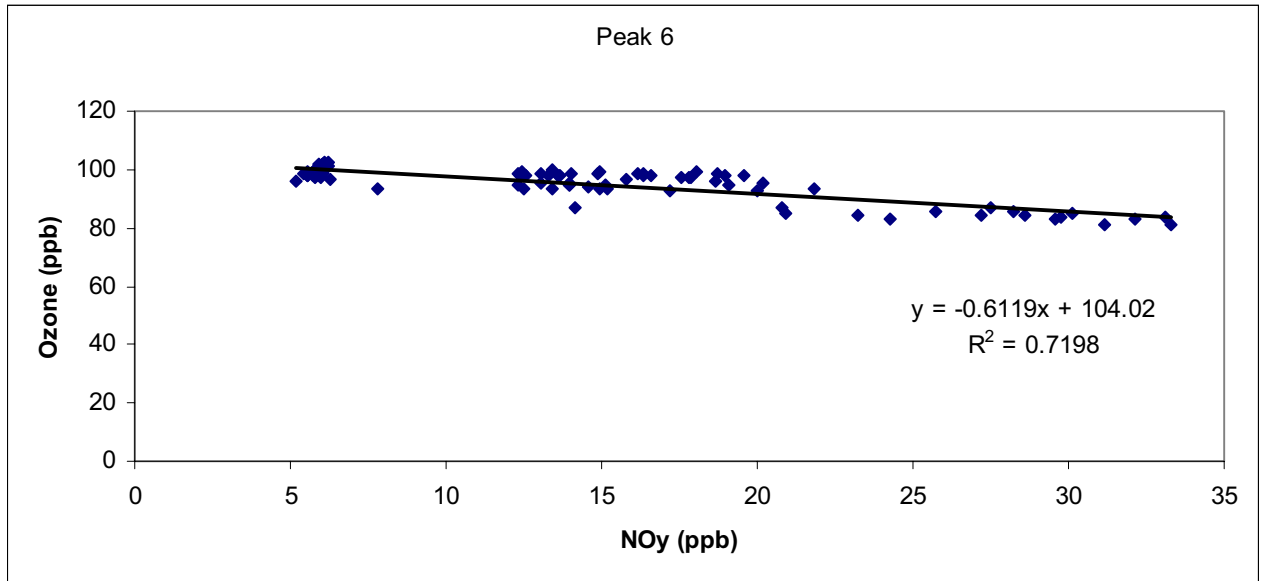


Figure 29. Scatter plots of ozone and SO₂ versus NO_y concentrations for peak 6.

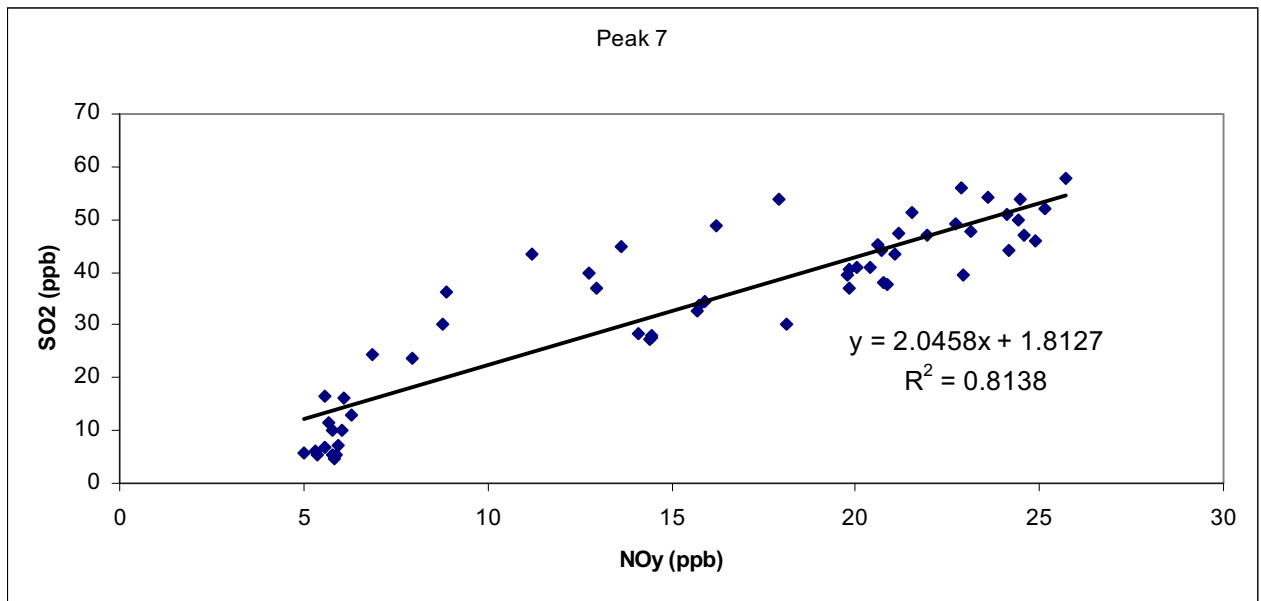
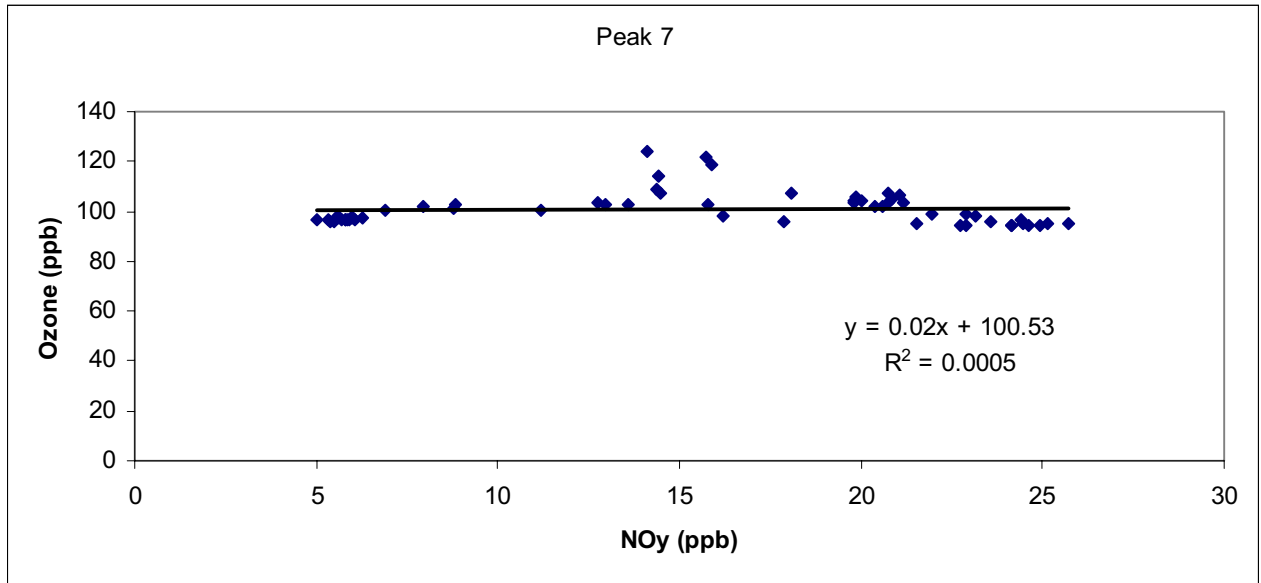


Figure 30. Scatter plots of ozone and SO₂ versus NO_y concentrations for peak 7.

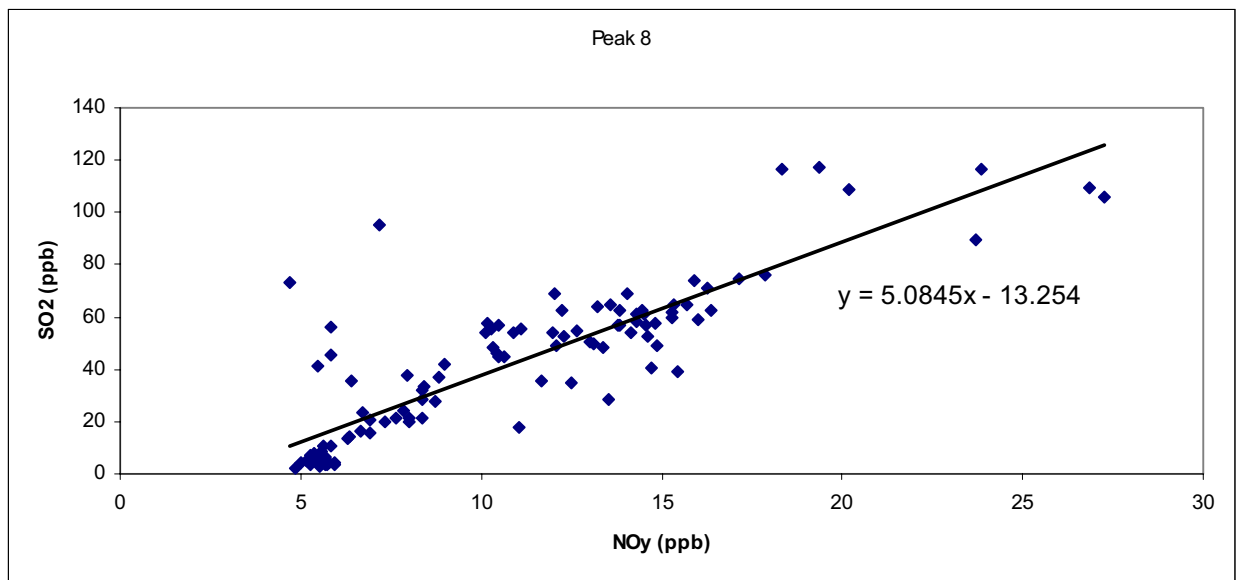
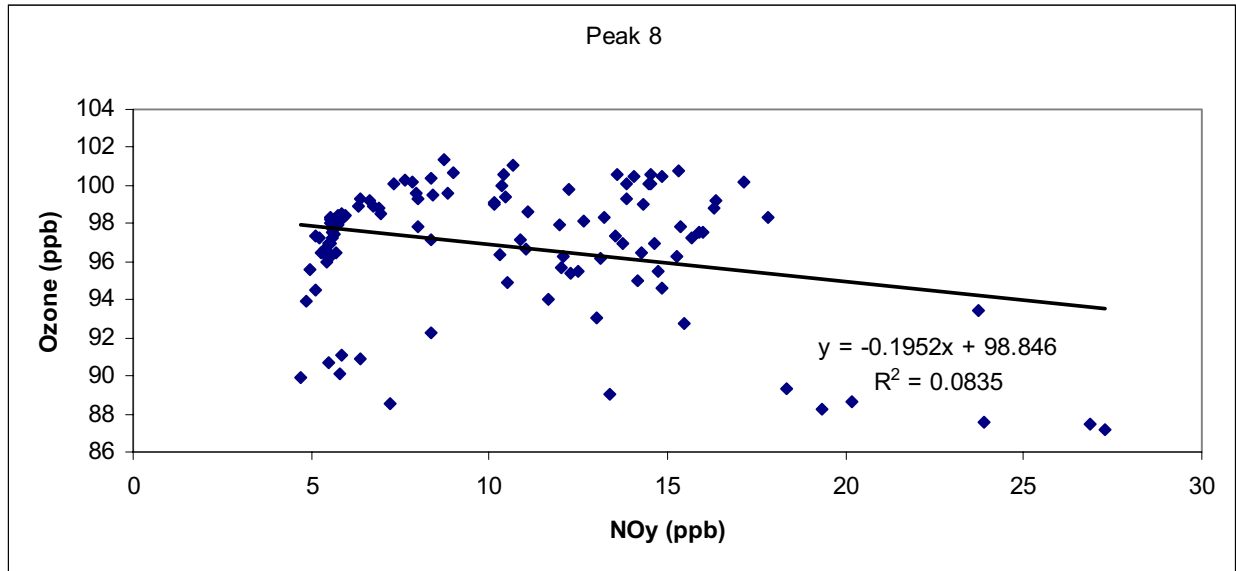


Figure 31. Scatter plots of ozone and SO₂ versus NO_y concentrations for peak 8.

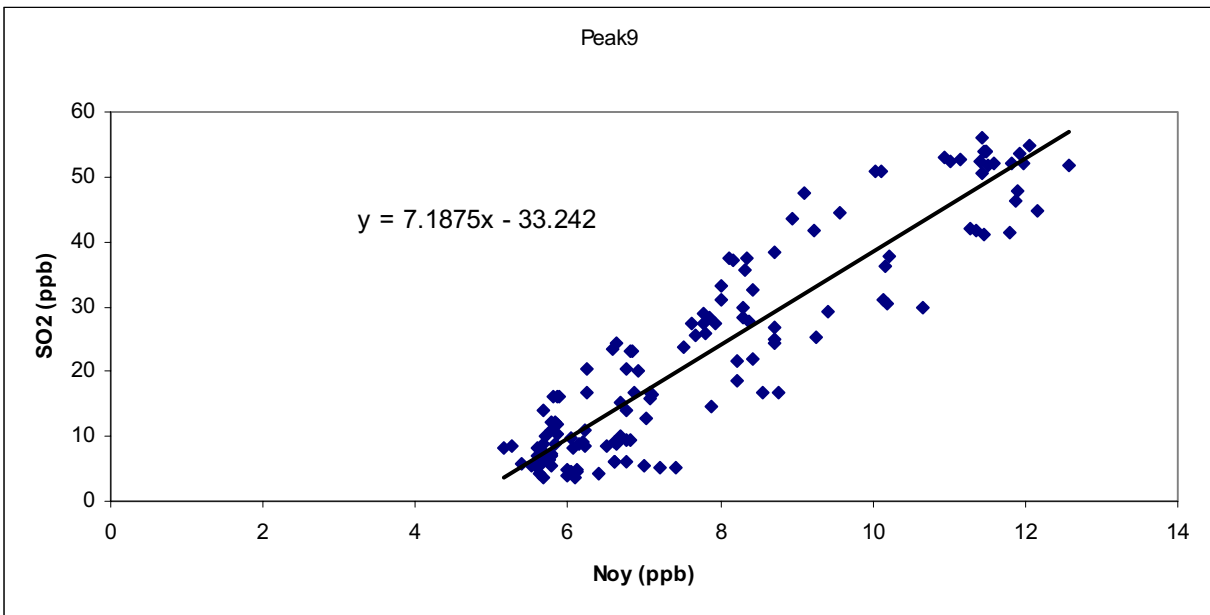
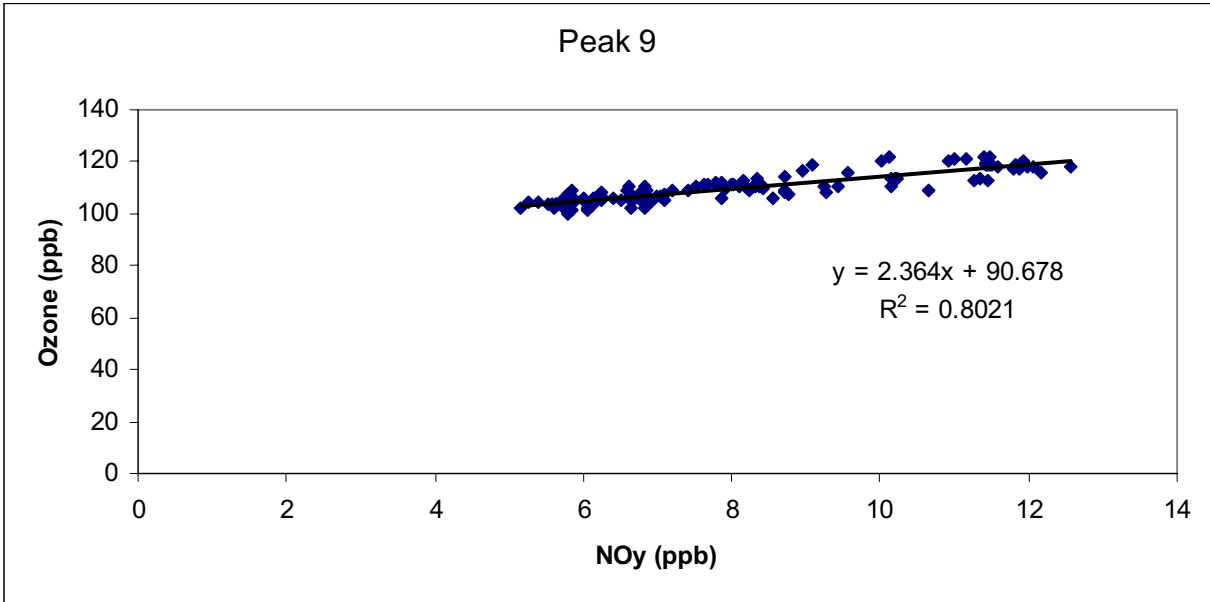


Figure 32. Scatter plots of ozone and SO₂ versus NO_y concentrations for peak 9.

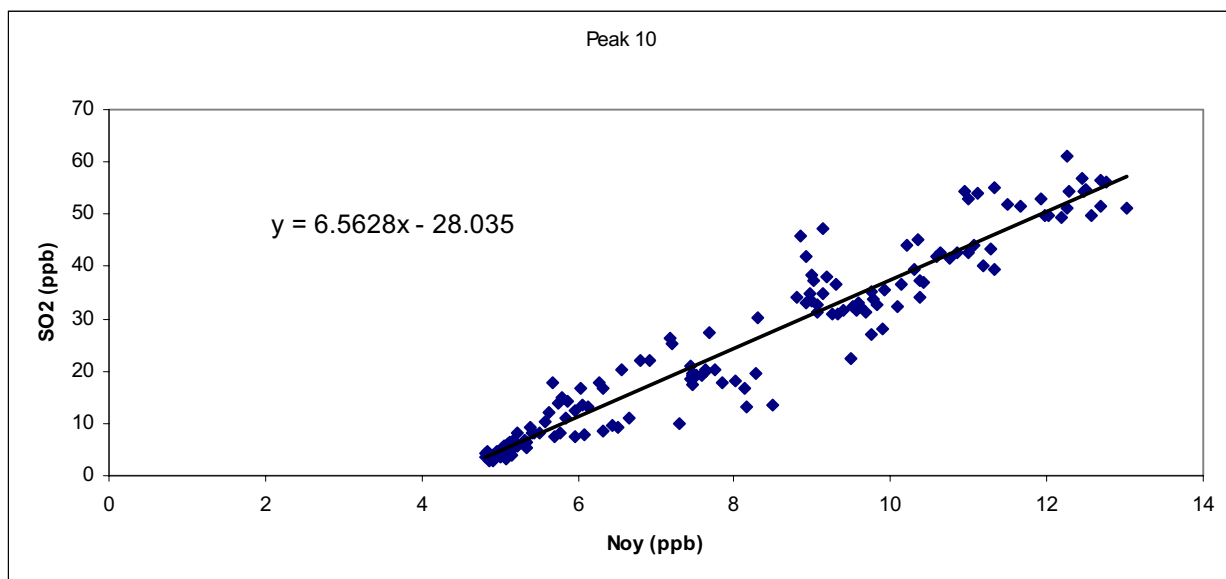
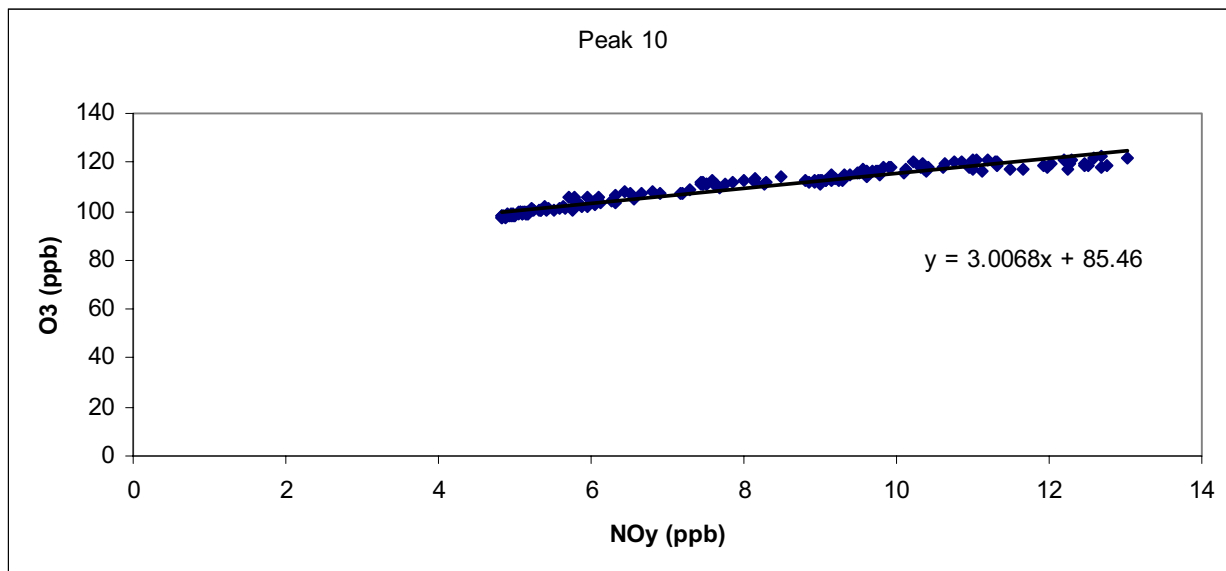


Figure 33. Scatter plots of ozone and SO₂ versus NO_y concentrations for peak 10.

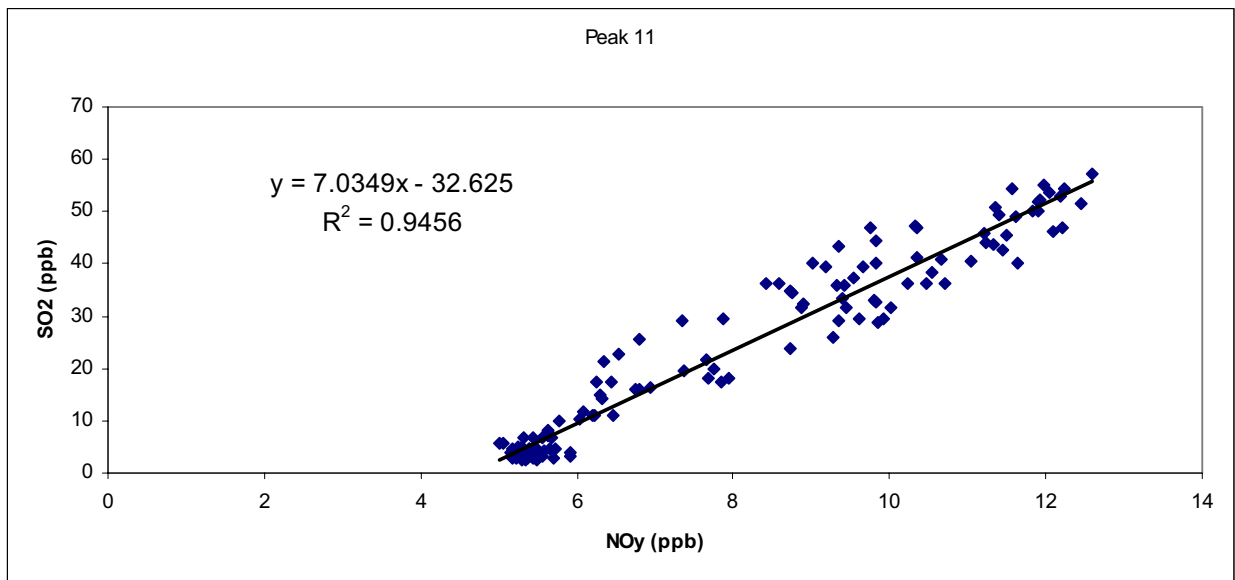
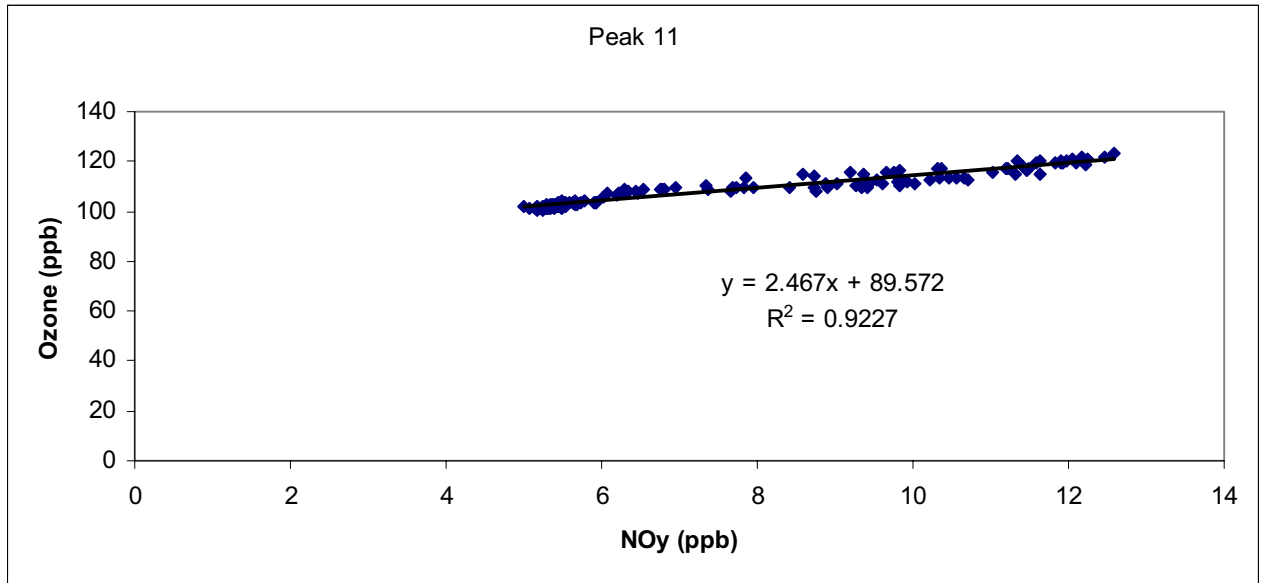


Figure 34. Scatter plots of ozone and SO₂ versus NO_y concentrations for peak 11.

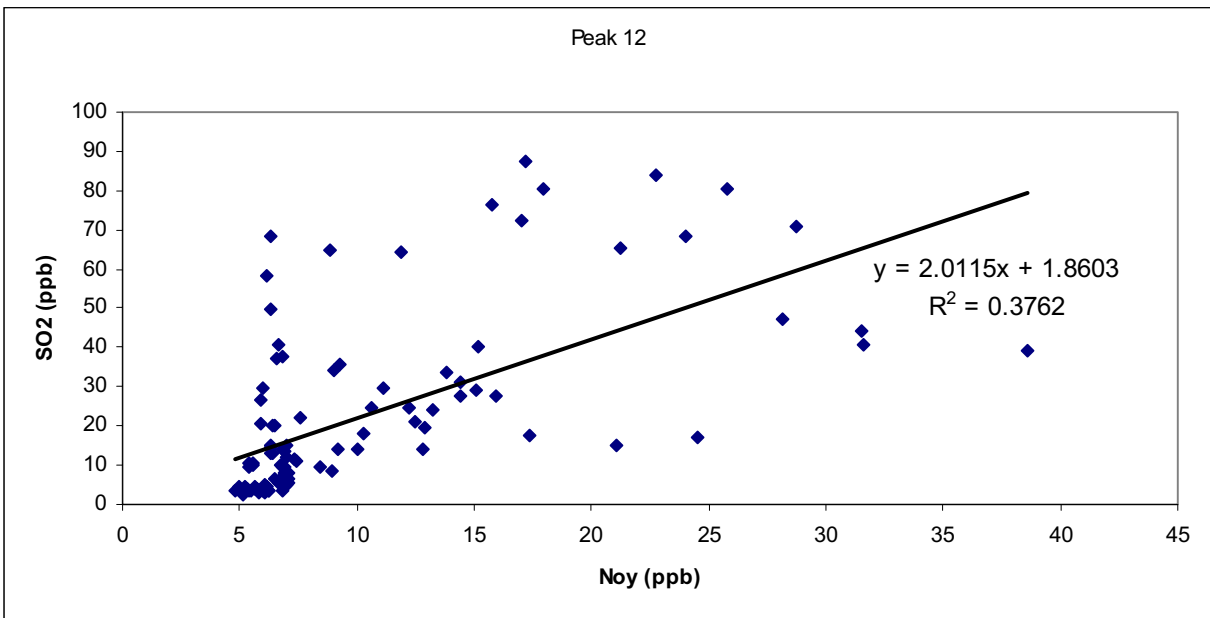
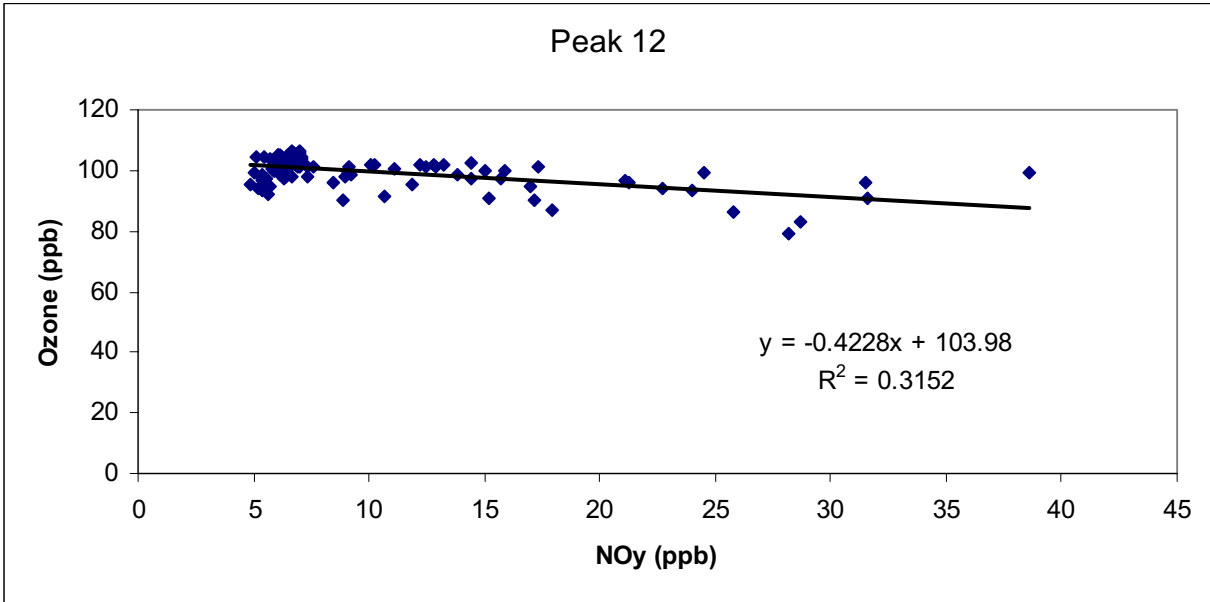


Figure 35. Scatter plots of ozone and SO₂ versus NO_y concentrations for peak 12.

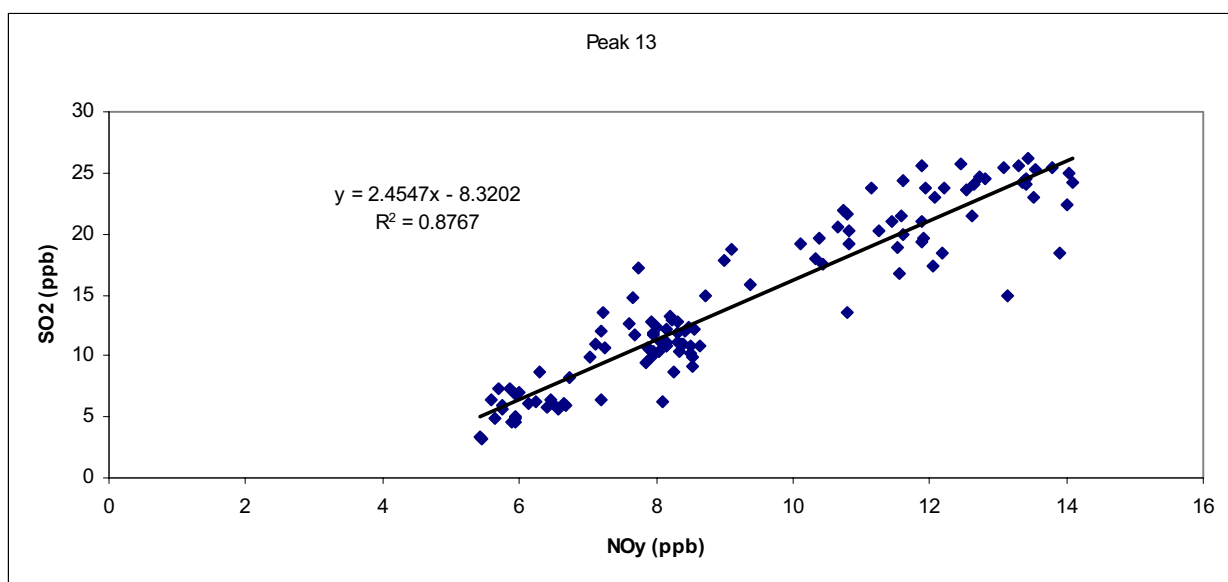
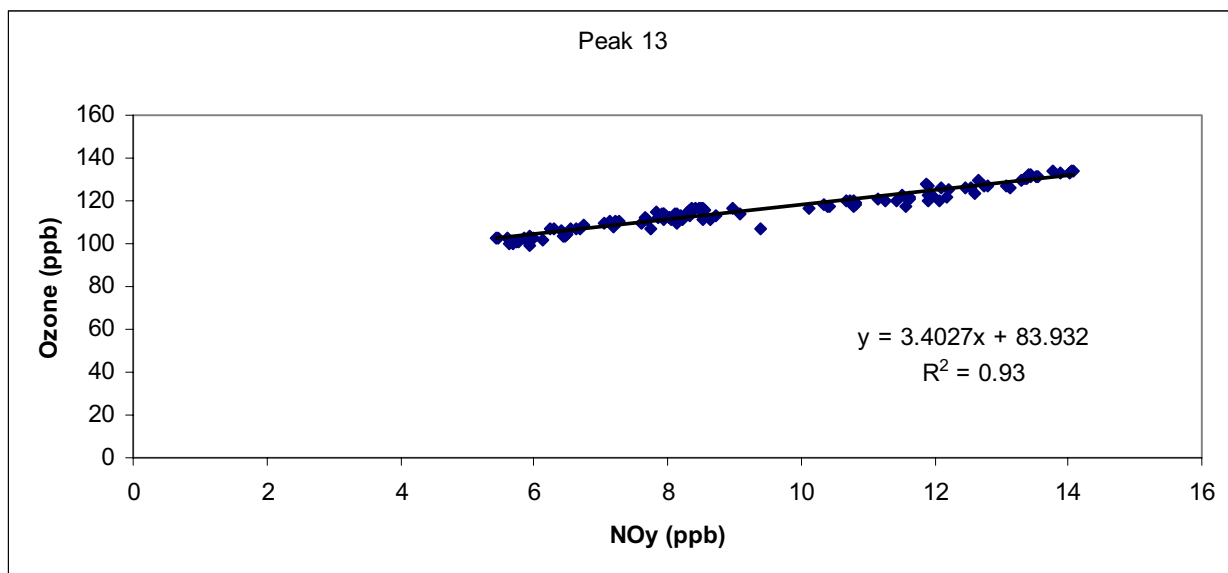


Figure 36. Scatter plots of ozone and SO₂ versus NO_y concentrations for peak 13.

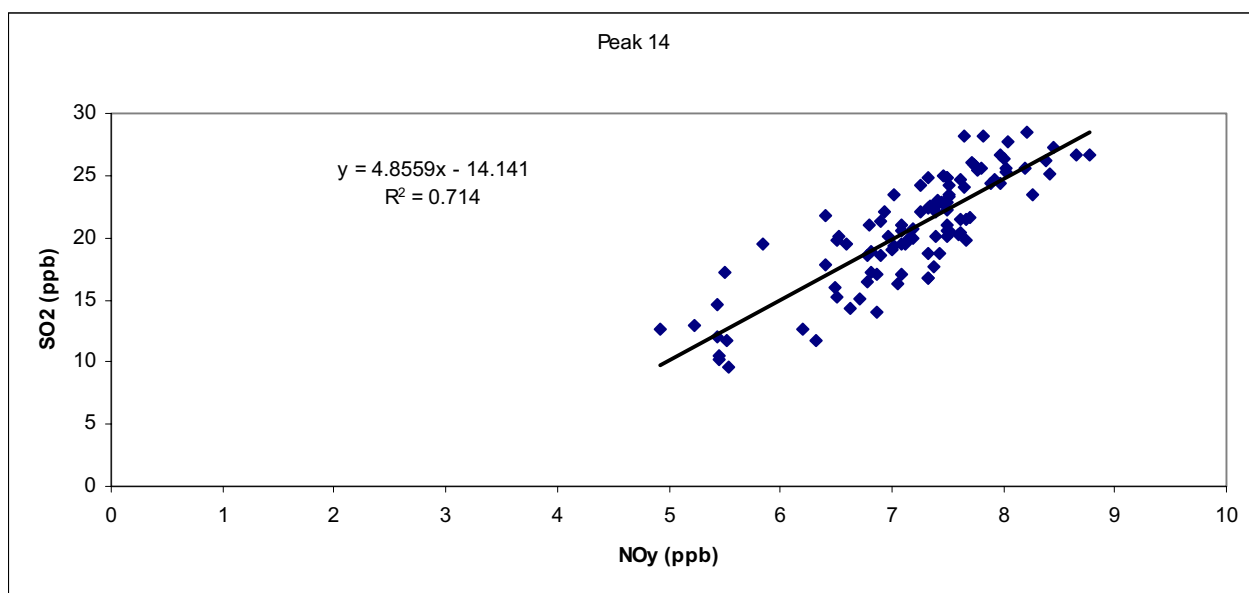
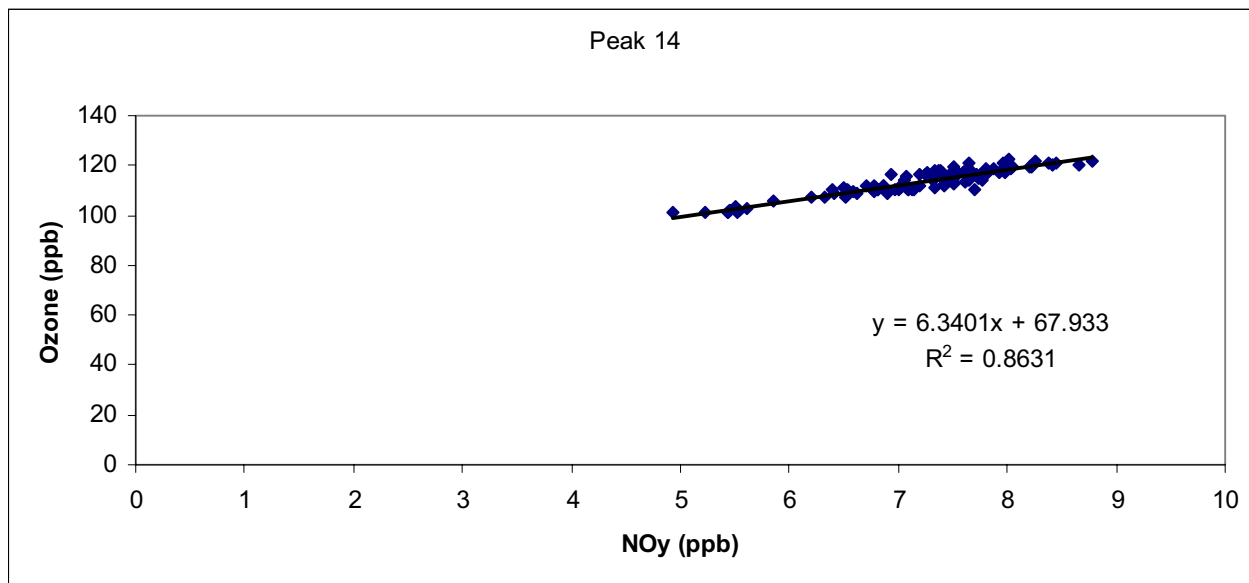


Figure 36. Scatter plots of ozone and SO₂ versus NO_y concentrations for peak 14.

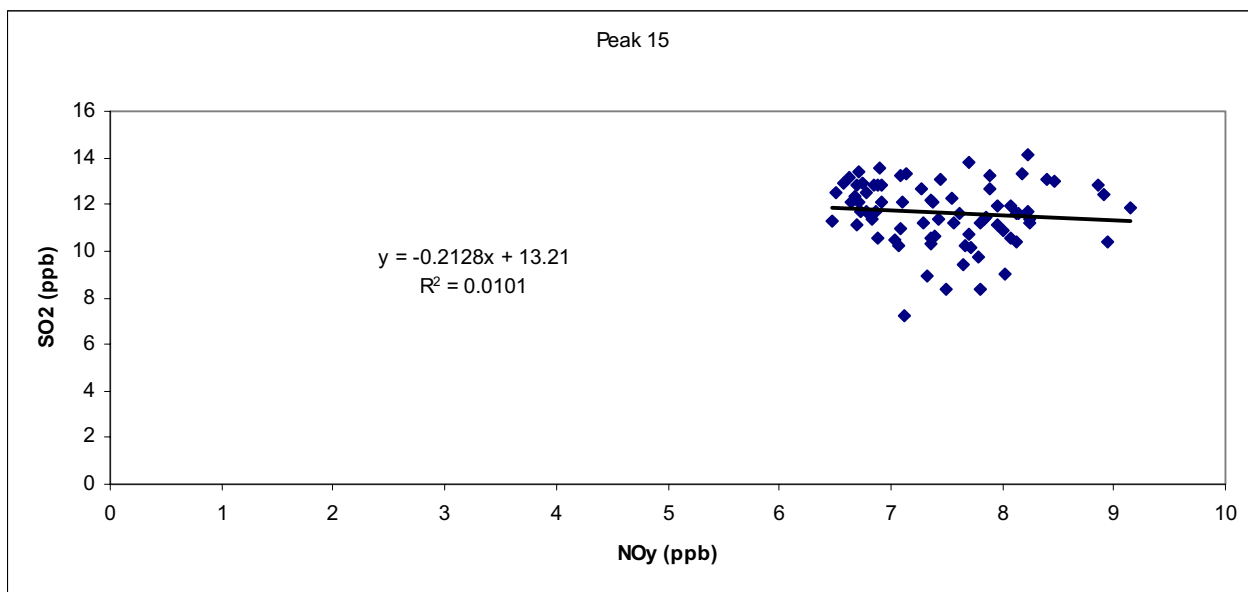
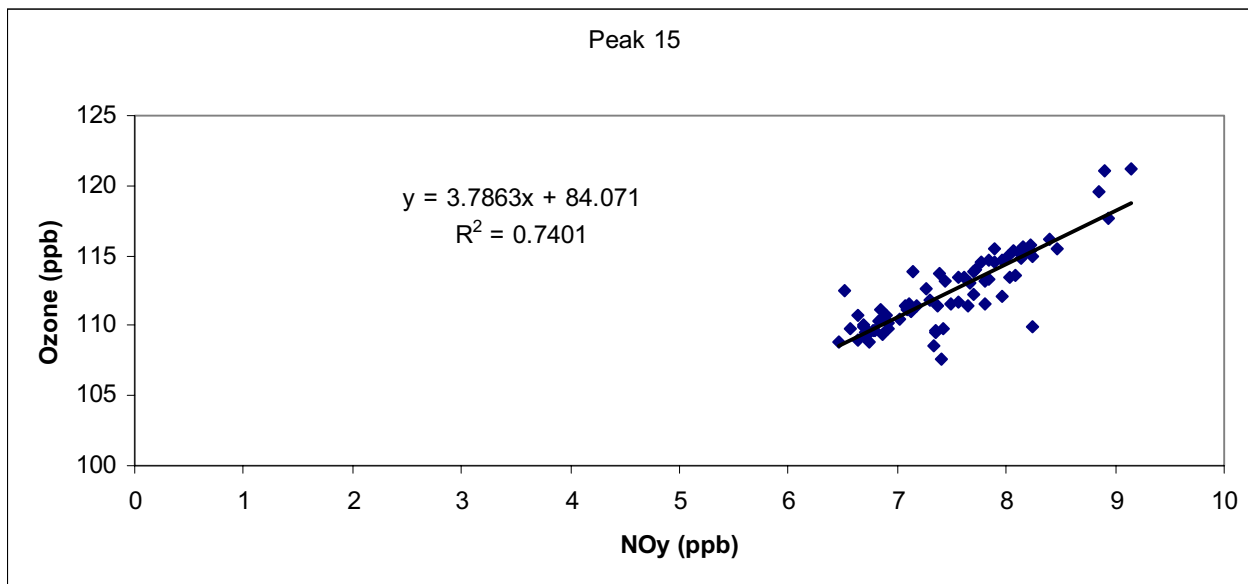


Figure 37. Scatter plots of ozone and SO₂ versus NO_y concentrations for peak 15.

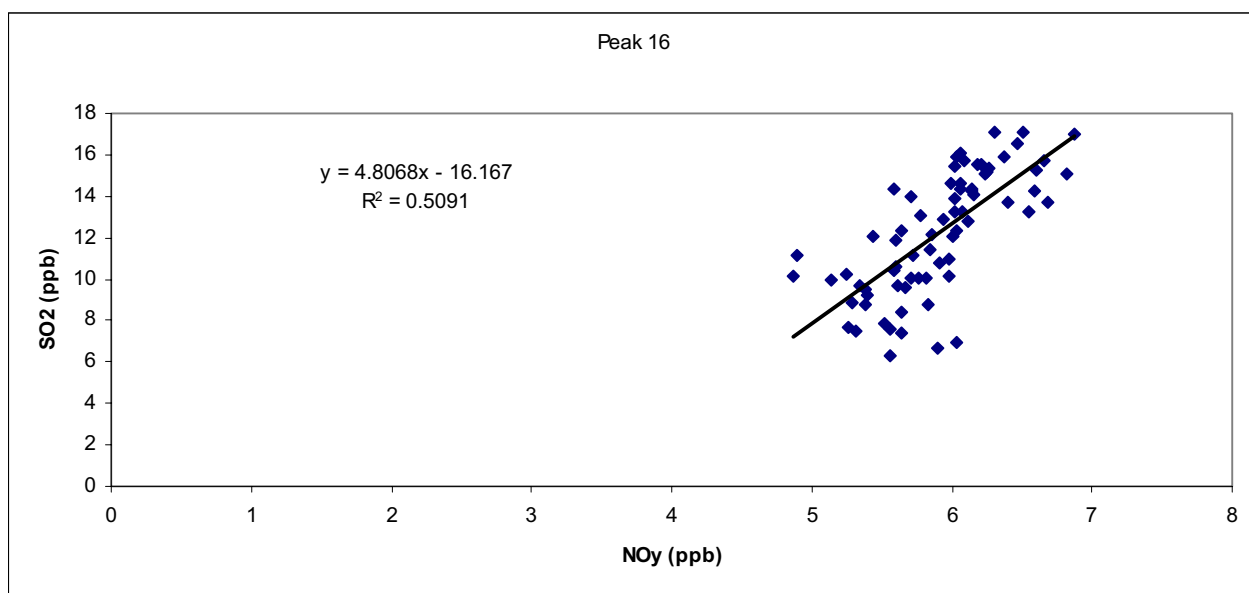
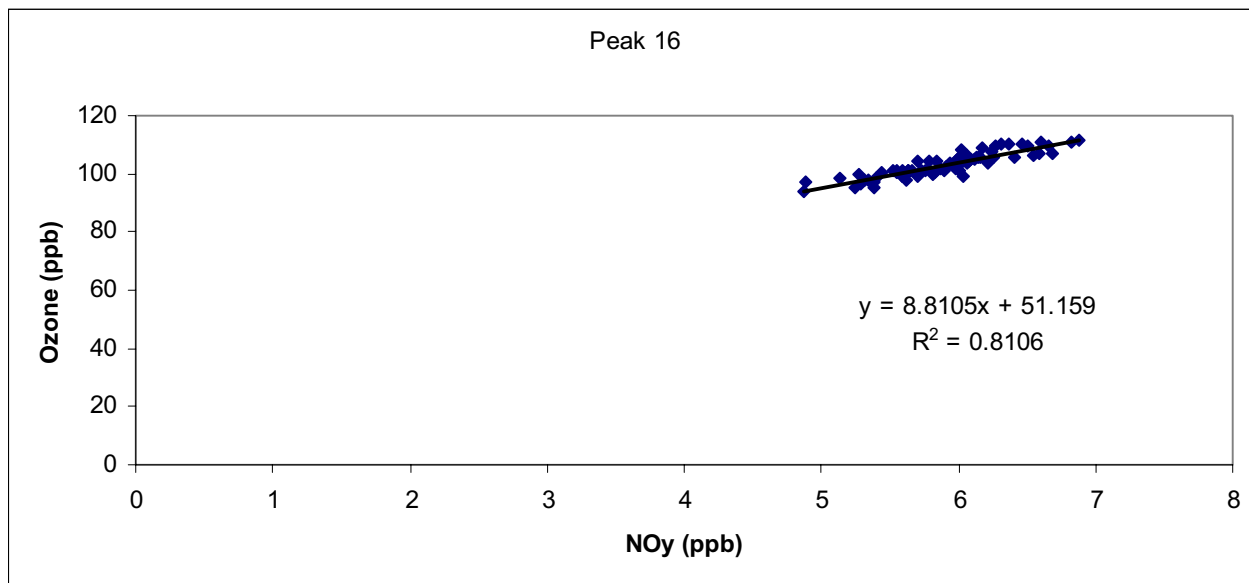


Figure 38. Scatter plots of ozone and SO₂ versus NO_y concentrations for peak 16.

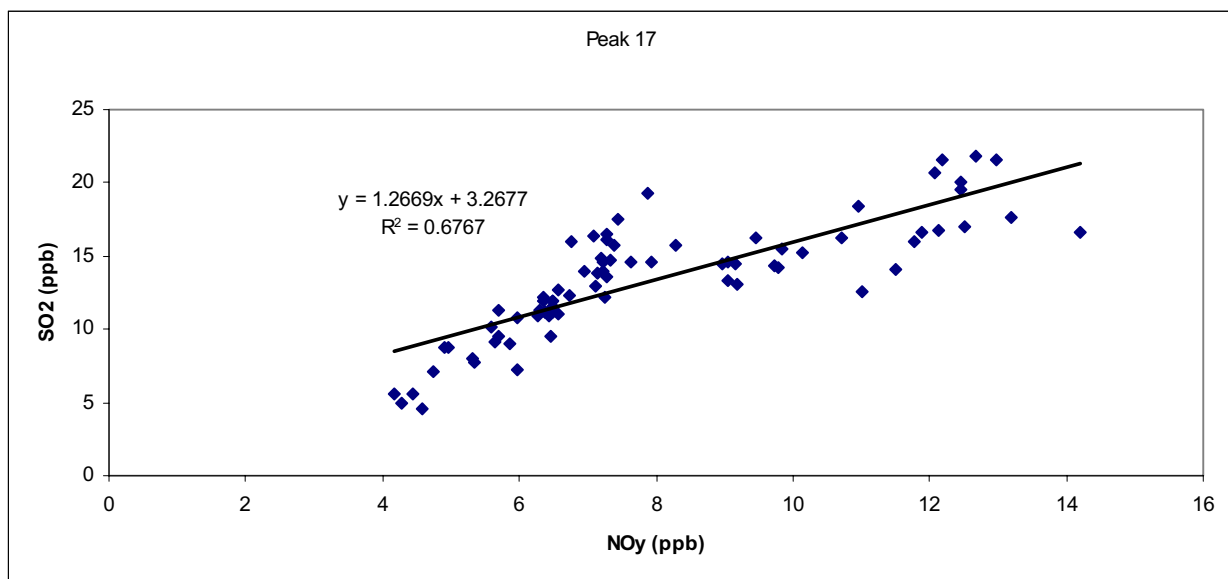
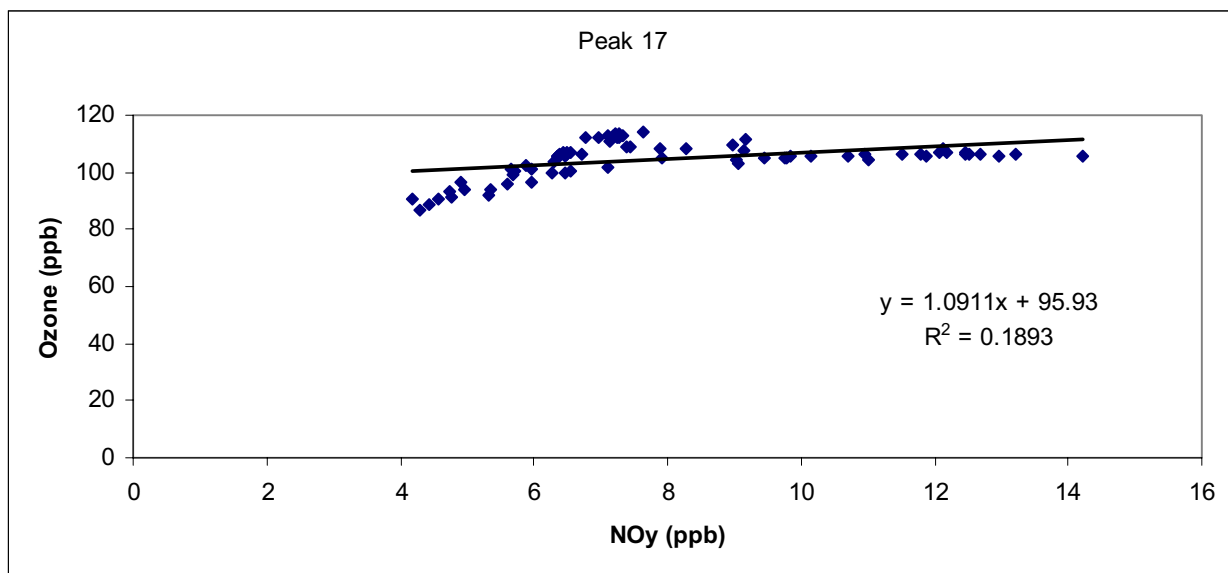


Figure 39. Scatter plots of ozone and SO₂ versus NO_y concentrations for peak 17.

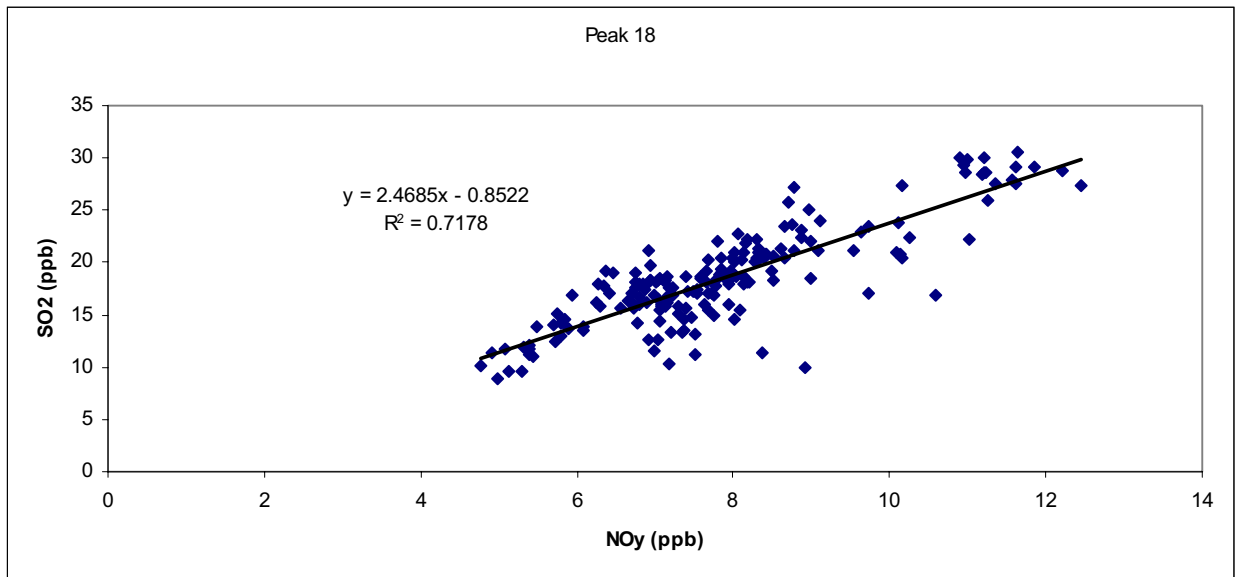
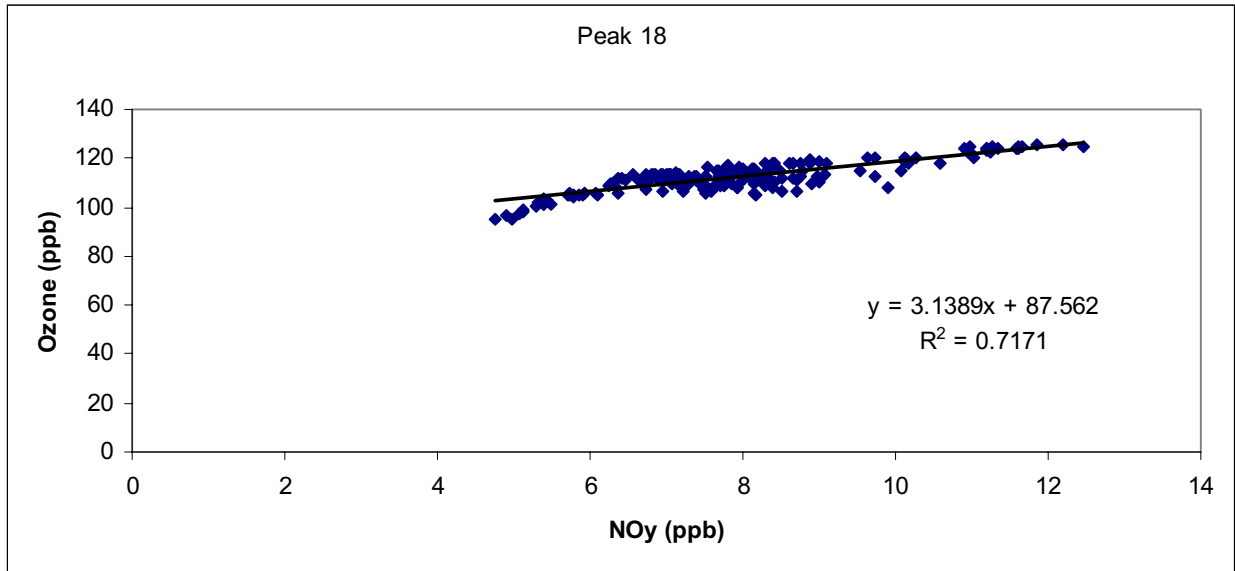


Figure 40. Scatter plots of ozone and SO₂ versus NO_y concentrations for peak 18.

Several factors were considered when determining the origin of these plumes including pollutant concentrations, wind direction, and the plane's location. Wind directions for this flight generally were from the north or northwest. This information coupled with the plane location suggested that peaks 2,5,6,7,8,9,10,11,14,16 and 18 were from the Monticello plant. Peaks 1,3,4,7,13,15, and 17 were traced to the Welsh Power plant and peak 12 originated from the Martin Lake power plant.

The following table gives the total tons of SO₂ that was emitted by the Welsh, Martin Lake, and Monticello power plants in September, October, and November of 2000. This data was taken from the U.S. EPA Emissions Tracking System (ETS) (www.epa.gov).

SO₂ emissions 3rd Quarter 2000	
Power plant	Total SO₂ emissions (Tons)
Welsh	11370
Monticello	26256
Martin Lake	16787

Based on the emission of SO₂ that each power plant reported in the 3rd quarter of 2000, the Monticello power plant was a higher emitter than Welsh or Martin Lake. This information was used to confirm the origin of each peak by comparing the SO₂/NO_y ratios collected by the aircraft. The peaks originating from the Monticello plant had larger SO₂/NO_y ratios when compared with the other peaks. The following table lists each SO₂ peak and their probable origin, time of encounter, and maximum ozone concentration.

SO₂ Peak	Probable Point Source	Time of peak encounter	Maximum Ozone Concentration (ppb)	Approximate Downwind Distance (km)	Approximate Downwind Time (hours)
1	Welsh	17:23:43 - 17:25:09	116	18	1.25
2	Monticello	17:28:14 - 17:27:33	107	23	1.6
3	Welsh	17:30:35 - 17:31:06	115	18	1.25
4	Welsh	17:37:17 - 17:38:50	113	18	1.25
5	Monticello	17:39:31 - 17:41:01	103	23	1.6
6	Monticello	17:45:19 - 17:46:57	102	23	1.6
7	Welsh	17:48:23 - 17:49:28	124	18	1.25
8	Monticello	17:50:25 - 17:52:18	101	23	1.6
9	Monticello	18:30:34 - 18:32:46	122	44	3.1
10	Monticello	18:43:29 - 18:44:02	123	44	3.1
11	Monticello	18:51:46 - 18:54:02	123	44	3.1
12	Martin Lake	19:37:18 - 19:39:01	106	9	0.6
13	Welsh	18:53:58 - 18:55:59	134	37	2.6
14	Monticello	19:07:59 - 19:09:43	122	63	4.4
15	Welsh	19:06:24 - 19:07:41	121	57	4.0
16	Monticello	19:25:33 - 19:26:50	111	95	6.6
17	Welsh	19:26:50 - 19:28:08	114	85	5.9
18	Monticello	19:34:03 - 19:37:18	125	112	7.8

During this flight the investigators aboard the aircraft collected in-situ VOC samples at 15-minute intervals. From these samples isoprene concentrations were determined. These concentrations, sampling times, and corresponding SO₂ peaks are listed in the following table.

Isoprene Conc. (ppb)	Sample Start Time	Sample End Time	Peak
0.049	9/3/2000 16:14	9/3/2000 16:15	N/A
0.035	9/3/2000 16:29	9/3/2000 16:30	N/A
0.039	9/3/2000 16:44	9/3/2000 16:45	N/A
0.457	9/3/2000 16:59	9/3/2000 17:00	N/A
2.558	9/3/2000 17:16	9/3/2000 17:17	N/A
1.093	9/3/2000 17:31	9/3/2000 17:32	3
1.778	9/3/2000 17:47	9/3/2000 17:48	7
0.044	9/3/2000 18:02	9/3/2000 18:03	N/A
0.068	9/3/2000 18:19	9/3/2000 18:19	N/A
0.746	9/3/2000 18:41	9/3/2000 18:42	10
0.455	9/3/2000 18:56	9/3/2000 18:57	13
0.482	9/3/2000 19:24	9/3/2000 19:25	16,17
0.581	9/3/2000 19:39	9/3/2000 19:40	12, 18
0.423	9/3/2000 20:00	9/3/2000 20:01	N/A
0.151	9/3/2000 20:17	9/3/2000 20:17	N/A
0.219	9/3/2000 20:33	9/3/2000 20:33	N/A
0.568	9/3/2000 20:49	9/3/2000 20:50	N/A
1.706	9/3/2000 21:04	9/3/2000 21:05	N/A
0.27	9/3/2000 21:19	9/3/2000 21:20	N/A
0.205	9/3/2000 21:49	9/3/2000 21:50	N/A

SUMMARY

Plumes were traced to power plants with a high degree of certainty due to consistent wind fields and matching signature SO₂ concentrations. The aircraft flew four transects at different distances downwind of the Welsh and Monticello plants allowing for observations of the plume at different ages. The episodes located in the first transect of these plume shows a decrease in ozone concentration due to high NO_x concentrations that are characteristic of young plumes. This phenomenon is also observed in the negative slopes of trend lines from the scatter plots of ozone vs. NO_y in peaks 1-8. As the plumes age subsequent transects show increases of ozone concentration and dilution of the SO₂. Again this is confirmed by the positive ozone efficiencies seen in the ozone vs. NO_y scatter plots of peaks 9-17.

Several of the peaks in the first transect (Peaks 1-8) show two SO₂ concentration spikes within each episode. This could be attributed to the instruments tracking multiple stacks

of different SO₂ concentrations at each power plant. This phenomenon could explain the large scatter of data observed in the SO₂ vs. NO_y plots in peaks 1-8. As the aircraft moved further away from the stacks the plume combined into one homogenous plume as observed in Peaks 9-17. This results in the decrease of scatter observed in the SO₂ vs. NO_y plots of those peaks.

The data from this flight have been studied to calculate the ozone productivities observed in these power plant plumes. These observed ozone productivities can be compared to ozone model results under similar meteorological conditions. The nature of the aircraft data will facilitate the comparison of the plumes at different ages and help evaluate model performance.